AIAA-2003-4676
39th AIAA/ASME/SAE/ASEE Joint Propulsion Conference and Exhibit, Huntsville Alabama, July 20-23, 2003

HOW TO BUILD AN ANTIMATTER ROCKET FOR INTERSTELLAR MISSIONS
- - - - -
SYSTEMS LEVEL CONSIDERATIONS IN DESIGNING ADVANCED PROPULSION TECHNOLOGY VEHICLES

Robert H. Frisbee
Jet Propulsion Laboratory, California Institute of Technology
4800 Oak Grove Drive, Mail Code 125-109
Pasadena CA 91109
Phone: (818) 354-9276 FAX: (818) 393-6682
E-Mail: robert.h.frisbee@jpl.nasa.gov

ABSTRACT

One of the few ways to do fast (ca. 0.5c cruise velocity) interstellar rendezvous missions is with a matter-antimatter annihilation propulsion system. This paper discusses the general mission requirements and system technologies that would be required to implement an antimatter propulsion system where a magnetic nozzle (superconducting magnet) is used to direct charged particles (from the annihilation of protons and antiprotons) to produce thrust. Scaling equations for the various system technologies are developed where, for example, system mass is a function of propulsion system power, and so on. With this data, it is possible to estimate total system masses. Finally, the scaling equations are treated parametrically to evaluate the sensitivity of changes in the performance of the various systems. For example, improvements in some system technologies can reduce the vehicle total (wet) mass by a significant amount; by contrast, changes in assumed performance in some systems can have negligible impact on overall mass, thereby providing a means for prioritizing technology development.

INTRODUCTION

One of mankind's oldest dreams has been to visit the tiny pinpoints of light visible in the night sky. Over the last 40 years we have visited most of the major bodies in our solar system, reaching out far beyond the orbit of Pluto with our robotic spacecraft. And yet this distance, which strains the limits of our technology, represents an almost negligible step towards the light-years that must be traversed to travel to the nearest stars. For example, even though the Voyager spacecraft is one of the fastest vehicles ever built, traveling at 17 km/s or 3.6 AU/year, it would still require almost 74,000 years for it to traverse the distance to our nearest stellar neighbor. Thus, travel to the stars is not impossible; it will, however, represent a major commitment by a civilization simply because of the size and scale of any technology designed to accelerate a vehicle to speeds of a few tenths of the speed of light.

The Vision Mission and Stretch Goal

For the purposes of evaluating the technologies required for a matter-antimatter annihilation propulsion system, we chose as our "Vision" mission a "fast" (0.5c cruise velocity), interstellar rendezvous mission. This represents a "stretch goal" that is intentionally made as difficult as possible so that a simple extrapolation of existing, near-term technologies would not suffice. Ultimately, this gives us a tool to aid in structuring future technology development programs and precursor missions with a long-range goal of giving us the capability to perform the Vision mission. As an historical example, we can consider the Apollo lunar landing as a Stretch Goal in the early 1960s. This led to development of technologies like large chemical rocket engines, fuel cells, and 0-gee cryogenic fluids systems. Similarly, it led to development during the Gemini Program of space operations techniques like rendezvous and docking. Finally, to support the human lunar landings, a number of robotic precursor missions like Ranger, Surveyor, and Lunar Orbiter were flown.

Previously, we have evaluated various propulsion options for interstellar missions to the nearest 1,000 stars, with missions ranging from 4.3 light years (LY) to 40 LY. Concepts considered included advanced electric propulsion, nuclear (fission, fusion, antimatter) propulsion, beamed energy (e.g., LaserSails, MagSails) propulsion, electromagnetic catapults, in-situ propellant production concepts (e.g., the interstellar ramjet), and hybrid systems (e.g.,

* Member AIAA

antimatter-catalyzed fission/ fusion). We found that for the most demanding stretch goal of a fast (e.g., 0.5 c), interstellar rendezvous mission only beamed energy Laser Sail, matter-antimatter, and fusion ramjet concepts were viable candidates.[1]

Technology Predictions

Predicting the types of systems and technologies to be used for an interstellar mission some 50-100 years from now is, somewhat by definition, virtually impossible. This is made obvious by considering the state of knowledge in 1903 versus 2003. For example, in 1903, Newton and Maxwell represented the reigning models of nature; advanced transportation technology was represented by Steam Locomotives (which at that time held the world speed record!). By contrast, 100 years later, Quantum Mechanics and Relativity rule physics; we have rockets, lasers, transistors, high-temperature (100K) super-conductors, and so on. The best we can do in extrapolating the future is stick to known physics, and try to extrapolate (guess!) what technology might do. Perhaps the most famous example is the difference between the dream of Jules Verne's From the Earth to the Moon (1865) and Apollo 11 (1969),[2] as illustrated in Table 1.

Table 1. Comparison between Jules Verne's Cannon and Projectile (1865) and the Apollo Saturn V and Command Module (1969).

System	Verne (1865)	Apollo (1969)
Launch Vehicle	**Cannon**	**Saturn V**
Height (m)	274	111
Diameter (m)	6.4	10.1
Mass (MT)	186,000	2,900
Max Accel. (gees)	22,000	5
Crew Capsule	**The Projectile**	**Command Module**
Crew	3	3
Height (m)	4.6	3.7
Diameter (m)	2.7	3.9
Mass (MT)	8.7	2,900
Useable Vol. (m^3)	6.5	5.6
Material	Aluminum	Aluminum

Verne was impossibly wrong in his prediction of the launch vehicle, yet he was remarkably right in predicting the crew capsule. In part, this is because of the quantum leaps in technological capability made by the launch vehicle (e.g., cannons versus rockets).[3] By contrast, the need to support three crewmembers in a trip to the Moon is somewhat technology-independent (i.e., they need a certain amount of living volume, food, oxygen, etc.), so it is perhaps not surprising that the crew capsules are so similar.

Antimatter Rocket Systems Analysis

This paper discusses the general mission requirements and system technologies that would be required to implement a "beam-core" antimatter propulsion system where a magnetic nozzle (superconducting magnet) is used to direct charged particles (pions from the annihilation of equal amounts of protons and antiprotons) to produce thrust. These systems include the Magnetic Nozzle (high-temperature [100 K] superconductor magnet), Radiation Shields (to protect the various spacecraft systems from the 200 MeV gamma-rays produced in the annihilation process), the Main Radiator (used to reject gamma-ray heat absorbed by the radiation shields) and other System Radiators (e.g., for the electric power system, refrigerators, etc.), Propellants (consisting of normal-matter liquid H_2 and antimatter in the form of solid anti-H_2), Propellant Storage and Feed System (tankage, insulation, feed system, etc.), Thermal Control Systems including propellant tank and superconductor magnet insulation and refrigerators (at 100 K for the superconductor magnet, 20 K for normal-matter liquid-H_2, and 1 K for solid anti-H_2), an Electric Power System (electric power for refrigerators, propellant feed system, etc.), Spacecraft Miscellaneous Systems (avionics, telecom, attitude control, etc.), the Payload (robotic), and, finally, a Dust Shield (to protect against interstellar dust impacts).

Particular emphasis is given to deriving scaling equations for the various system technologies as, for example, mass as a function of propulsion system power, and so on. With this data, it is possible to estimate total system masses. Finally, the scaling equations are treated parametrically to evaluate the sensitivity of changes in the performance of the various systems; for example, a 10-fold improvement in superconductor magnet critical current density, I_o, from today's $1x10^{10}$ Amps/m^2 to $1x10^{11}$ Amps/m^2 can reduce the vehicle total (wet) mass by a factor of about two. By contrast, changes in assumed performance in some systems can have negligible impact on overall mass, thereby providing a means for prioritizing technology development.

MISSION ANALYSIS

The long-range mission goal is the ability to rendezvous with scientifically interesting planets circling about other stars. Mission targets, such as planets capable of harboring life (and, ultimately, planets habitable by humans), would be identified by the NASA Origins Program, which has the long-range goal (by ca. 2040) of detecting, remote-sensing spectral analysis, and imaging of potentially habitable planets around stars out to ~ 40 LY (nearest 1,000 stars). This will be accomplished by the use of progressively more sophisticated space-based observational techniques

(e.g., telescopes, interferometers, etc.) to ultimately image Earth-like planets in the potentially habitable region – the "Goldilocks Zone": not too hot, not too cold – about a star.

Robotic interstellar missions can be viewed as a natural follow-on to the Origins Program; the Origins Program will tell us where to send the interstellar spacecraft that will provide close-up imaging with a flyby, and detailed in-situ science (ground truth) with a rendezvous missions. Current emphasis on a fast interstellar rendezvous mission where the spacecraft stops at its destination. Thus, there is a desire for a high cruise velocity to minimize trip time. For example, to travel 4.3 LY with a 10 year trip time requires an average speed of 0.43 c. However, a high-speed (≥0.1 c) flyby is not thought to give significantly more science return than that provided by Origins Program capability in the time frame of interest; in effect, virtually as much imaging capability is provided by advanced telescopes at Earth as from a rapidly moving spacecraft in a flyby (e.g., a flythrough of our Solar System would only allow 110 hours of observation at 0.1 c). Thus we see the need for a rendezvous mission, even though this has the effect of doubling the mission ΔV.

For the purposes of sizing the antimatter rocket, we will assume a need to reach a cruise velocity of 0.5 c. However, trip time is a function of acceleration as well as cruise velocity. For example, too low an acceleration can adversely impact trip time, because the vehicle spends too much time in the acceleration/deceleration phase and not enough time at peak (cruise) velocity. As shown in Figure 1, in order to minimize the trip time (by maximizing the time spent at peak velocity), the vehicle needs to accelerate (and decelerate) at 0.01 gee (1 gee = 9.8 m/s^2 = 1.03 LY/Yr^2) as a minimum. Higher acceleration is better, but higher acceleration also requires more power (and vehicle systems mass). Interestingly, there is no significant benefit for acceleration > 1 gee.

The difficulty is that, as we will see below, an antimatter rocket is severely acceleration-limited because of its high specific impulse (I_{sp} ~ 10 million lb_f-s/lb_m, or 0.33 c). The interaction between engine "jet" power (P_{jet}, Watts), I_{sp}, and thrust (F, Newtons) is given by:

$$P_{jet} = 1/2\ g_c\ I_{sp}\ F \qquad \text{(Eq. 1)}$$

where I_{sp} in common units of lb_f-s/lb_m is converted to exhaust velocity units (m/s) by multiplying by g_c = 9.8 m/s^2. The companion equation for specific impulse is:

$$g_c\ I_{sp} = F / \text{M-DOT} \qquad \text{(Eq. 2)}$$

where M-DOT is the flow rate (kg/s) of propellant into the engine. Acceleration is often defined in terms of the thrust-to-weight (T/W) ratio of the vehicle; in this case, thrust (force) divided by weight is proportional to (P_{jet}/I_{sp}) / (Mass). However, because of its large I_{sp}, an antimatter rocket requires an enormous jet power to produce any thrust, but the mass also grows rapidly as power increases. For example, as shown below, an antimatter rocket with an acceleration (T/W) of 0.03 gees is roughly 16 times heavier than a T/W=0.01 gee vehicle. Thus, for purposes of sizing the vehicle, we will assume a "nominal" T/W of 0.01 gee for all stages in the antimatter rocket, and iteratively calculate the corresponding P_{jet}, M-DOT, thrust, and ultimate vehicle mass.

MATTER-ANTIMATTER ANNIHILATION

Matter-antimatter annihilation offers the highest possible physical energy density of any known reaction substance. The ideal energy density ($E/M=c^2$) of $9x10^{16}$ J/kg is orders of magnitude greater than chemical ($1x10^7$ J/kg), fission ($8x10^{13}$ J/kg), or even fusion ($3x10^{14}$ J/kg) reactions. Additionally, the matter-antimatter annihilation reaction proceeds spontaneously, therefore not requiring massive or complicated reactor systems. These properties (high energy density and spontaneous annihilation) make antimatter very attractive for propulsively ambitious space missions (e.g., interstellar travel).

Antimatter for Propulsion Applications

Note that for a propulsion application, proton-antiproton annihilation is preferred over electron-positron (anti-electron) annihilation because the products of proton-antiproton annihilation are charged particles that can be confined and directed magnetically. (The antiproton is identical in mass to the proton but opposite in electric charge and other quantum numbers.) By contrast, electron-positron annihilation produces only high-energy gamma rays, which cannot be directed to produce thrust and do not "couple" their energy efficiently to a working fluid (and also require significant shielding to protect the vehicle and its payload). This is the primary reason for selecting the annihilation of a proton (p^+) and antiproton (p^-); the products include neutral and charged pions (π^o, π^+, π^-), and the charged pions can be trapped and directed by magnetic fields to produce thrust. However, the pions produced in the annihilation reaction do possess (rest) mass (about 22% of the initial proton-antiproton annihilation pair rest mass for charged pions, 14% for the neutral pions), so not all of the proton-antiproton mass is converted into energy. This results in an energy density of the proton-antiproton reaction of "only" 64% of the ideal limit, or $5.8x10^{16}$ J/kg. A summary of the distribution of mass-energy in the annihilation reaction between an anti-proton and positron and their normal-matter counterparts is shown in Table 2.

Table 2. Matter-Antimatter Annihilation Product Distribution.

Species	Rest Mass (MeV)	Fraction of Total (%)	Kinetic Energy (MeV)	Fraction of Total (%)	Total Mass-Energy (MeV)	Fraction of Total (%)
Initial Reactants						
P+	938.3	49.97	0	0	938.3	49.97
e-	0.5	0.03	0	0	0.5	0.03
P-	938.3	49.97	0	0	938.3	49.97
e+	0.5	0.03	0	0	0.5	0.03
Initial Products						
2.0 π^o	269.9	14.38	439.1	23.39	709.1	37.77
1.5 π+	209.4	11.15	374.3	19.94	583.7	31.09
1.5 π-	209.4	11.15	374.3	19.94	583.7	31.09
e- + e+ -> 2 γ			1.0	0.05	1.0	0.05
Decay Products						
2.0 π^o -> 4 γ			709.1	37.77	709.1	37.77
1.5 π+ -> 1.5 μ+	158.5	8.44	288.5	15.36	446.9	23.80
1.5 π+ -> 1.5 ν_m			136.8	7.28	136.8	7.28
1.5 π- -> 1.5 μ-	158.5	8.44	288.5	15.36	446.9	23.80
1.5 π- -> 1.5 anti-ν_m			136.8	7.28	136.8	7.28

One serious issue is the gamma radiation produced in the annihilation reaction. Because of the short (relativistic) lifetime of the neutral pion, it only moves 0.06 micrometers before decaying into gammas.[4] In practical terms, this means that the neutral pions promptly decay into very high-energy gamma rays (ca. 200 MeV each) at the annihilation point. By contrast, the charged pions move 21 m and their decay products, charged muons, move another 1.85 km before decaying.[4] Thus, one major systems consideration in designing a proton-antiproton annihilation propulsion system is the need to shield spacecraft systems against an intense (e.g., 38% of the propellant mass), high-energy flux of gamma radiation. (By comparison, the electron-positron annihilation gammas, at 0.511 MeV each, are negligible.) Finally, we have treated the annihilation mass-energy distribution as if it were possible to separate out rest mass from kinetic energy; in fact, of course, we must deal with the relativistic mass-energy content (e.g., rest mass plus relativistic mass "increase" due to traveling at >0.9 c) of the pions, etc. Thus, for example, the total mass-energy content of the neutral pion is converted into gammas, not just its rest mass.

For these reasons, antimatter for propulsion applications is typically assumed to be in the form of antiprotons, neutral antihydrogen atoms (an antiproton with a positron), or anti-molecular hydrogen (anti-H_2). Antiprotons do not exist in nature and currently are produced only by energetic particle collisions conducted at large accelerator facilities (e.g., Fermi National Accelerator Laboratory, FermiLab, in the U.S., CERN in Geneva Switzerland, or IHEP in Russia). This process typically involves accelerating protons to relativistic velocities (very near the speed of light) and slamming them into a metal (e.g., tungsten) target. The high-energy protons are slowed or stopped by collisions with nuclei of the target; the relativistic kinetic energy of the rapidly moving antiprotons (more correctly the relativistic mass increase due to traveling near the speed of light) is converted into matter in the form of various subatomic particles, some of which are antiprotons. The antiprotons are electromagnetically separated from the other particles. Note that antiprotons annihilate spontaneously when brought into contact with normal matter; thus, they must be contained by electromagnetic fields in high vacuums. This greatly complicates the collection, storage and handling of antimatter.

Currently the highest antiproton production level (not optimized for rate or efficiency) is of-the-order-of 10^{16} antiprotons or 10 nanograms (ng) per year, although planned upgrades to CERN may increase these production rates by a factor of 10-100. Additionally, only a much lower level of antiprotons have actually been collected, cooled, and stored after production. Finally, current production technology has an energy efficiency of only about 1 part in 10^9 (i.e., 10^9 units of energy are consumed to produce an amount of antimatter that will release one unit of energy upon annihilation).[4]

Portable antiproton traps are being developed for near-term research applications that would allow filling of the trap at an antiproton production facility (e.g., CERN, FermiLab) and transporting the stored antiprotons to a remote research facility. Pennsylvania State University (PSU) completed a Mark I portable antiproton Penning Trap in 1999. It was designed to hold ~10^{10} antiprotons. An improved Mark II Penning Trap (with a 100-fold higher capacity) is currently under construction at NASA Marshall Spaceflight Center (MSFC).

Antimatter Storage as High-Density Solid Anti-H_2

The technology of scaling production,

collection and cooling rates up to the levels required by space missions is still very much in the future. Additionally, the question of high-density storage of antimatter has not been answered. Current concepts for antimatter storage include storing it as neutral anti-molecular hydrogen (anti-H_2) ice suspended in an electromagnetic trap, as slightly charged cluster-ions suspended in an electromagnetic trap, and as individual antiprotons stored at quasi-stable lattice points in solid-state crystals. For this study, we have assumed storage as solid anti-H_2 in a magnetic trap.

More generally, we have a need to store large amounts of antimatter in a "non-contact" storage system. In principle, we could store the antiprotons on the vehicle using the same techniques used today; i.e., as a low density space-charge limited antiproton ion "gas." However, as shown in Figure 2, the typical space-charge limit of around 10^{11} ions/cm^3 results in an unrealistically large volume for even small numbers of antiprotons (e.g., milligrams of antiprotons would occupy a volume comparable to the Space Shuttle External Tank [ET]). This drives us towards storing antiprotons as condensed-phase liquid or solid anti-molecular hydrogen (anti-LH_2 or anti-SH_2); for example, the Shuttle ET could store in excess of 100 metric tons (MT) of liquid hydrogen. Interestingly, it is reasonable to imagine storing small amounts of antiproton ions for use in near-term space propulsion applications where small amounts of antiprotons are required, such as antiproton-catalyzed micro-fission/fusion.[5]

The requirement for production and storage of antimatter as high-density condensed-phase (liquid or solid) molecular H_2 represents a major feasibility issue (and is a potential show-stopper). Only the initial step of converting antiprotons (and positrons) into anti-H atoms has been demonstrated in the laboratory. The remaining steps of converting anti-atoms into anti-H_2 gas molecules and then into liquid/solid anti-H_2 have yet to be demonstrated, although some of these steps have been demonstrated for other atoms (but not for hydrogen) using "non-contact" approaches (e.g., "laser" cooling).

If production of anti-H_2 can be achieved, the solid or liquid anti-H_2 can be stored (levitated) magnetically (LH_2 and SH_2 are diamagnetic) to avoid contact with normal-matter walls, etc. This has already bee demonstrated for normal-matter LH_2 and SH_2 droplets.[6] A schematic of the "sombrero" shaped magnetic field used in these experiments is shown in Figure 3. These experiments also showed that it was possible to move individual drops around the field ring by means of both electrostatically charged and electromagnetic probes.

Finally, there will be a need to store the anti-H_2 as a very cold (1-2 K) solid to prevent evaporation (sublimation), because gaseous (anti) H_2 can't be contained magnetically and would drift to the storage container walls and annihilate. As a practical consideration, the anti-SH_2 would be stored as individual small solid pellets to facilitate extraction and feed into engine. This would result in a significantly lower "effective" density than that of the bulk solid (e.g., we will assume ~1/10 solid density).

Antiproton Production Issues

Eventually, there will be a need to produce enormous amounts of solid anti-H_2 for interstellar rendezvous missions. However, current world production of antiprotons is only on the order 10 ng per year. Current and near-term quantities will allow researchers to perform basic physics and engineering experiments, and, eventually, sub-scale thruster tests for brief durations. However, note that today's facilities are basic research laboratories, not "factories." As research facilities, their experimental need for precisely controlled momentum (angle and velocity) states limits acceptance (antiproton capture) to a small fraction of the total produced. Numerous options for improvements in number and efficiency have been discussed. Nevertheless, any discussion of antimatter propulsion must contend with the difficulty and cost of its production.

In this respect, it is interesting to compare the historical growth in the production rate of antimatter (specifically antiprotons) with that of liquid hydrogen (LH_2), as shown in Figure 4. James Dewar liquefied the first few drops of liquid hydrogen in 1898; today, every Space Shuttle launch consumes 100 MT of LH_2. With ten Shuttle flights per year, this implies a roughly 100-billion-fold (10^{11}) increase in the annual production and consumption of LH_2 for space applications alone in the roughly 80 years between liquid hydrogen's first production and its extensive use for Shuttle operations. For comparison, we have already had a 10^{16} increase in antiproton production rate in only 45 years, suggesting that significant advances may be possible in this area (e.g., another 45 years at this rate of growth would represent a production rate of thousands of tons per year).

Antimatter Propulsion and the Rocket Equation

The classical Rocket Equation relates the "dry" mass (M_b) and "wet" mass (M_o) (with propellant, M_p) of a rocket to the velocity change (ΔV) and specific impulse (I_{sp}) of the propulsion system:

$$M_o / M_b = \exp (\Delta V / I_{sp}) \qquad \text{(Eq. 3)}$$

(For convenience, we have assumed that I_{sp} is in velocity units compatible with ΔV.)

One interesting consequence of the "loss" of roughly 78% of the initial propellant mass (i.e., only 22% of the initial propellant mass appears as charged

pion mass) is that the Rocket Equation no longer holds. This is because only 22% of the initial mass of propellant in the rocket is available to produce the momentum that drives the rocket forward. (It is as if you designed a rocket that expelled 78% of the propellant mass sideways, perpendicular to the vehicle velocity, in a fashion that cancelled out any sideways motion and contributed nothing to the forward motion of the rocket.) This effect represents a major impact to the Rocket Equation. Also, it is necessary to use a Relativistic Rocket Equation that takes into account the relativistic effects of both the vehicle and propellant exhaust (charged pions) moving near the speed of light. These two modifications results in a mass ratio (M_o/M_b) for a given ΔV and I_{sp} that is much higher for a relativistic matter-antimatter rocket (with "loss" of propellant) than for either a classical or relativistic "conventional" rocket (where only a small amount of propellant mass is converted into energy).

A full derivation of the classical, relativistic, classical antimatter (i.e., with loss of propellant), and relativistic antimatter Rocket Equation has been given previously;[1] the relativistic antimatter Rocket Equation is summarized below.

The derivative form of the equation is:

$$dM_r / M_r = -dV(1- I_{sp}V/c^2)/\{(1-V^2/c^2)(- I_{sp}/c^2V^2+(1-a)V+a\, I_{sp})\} \quad \text{(Eq. 4)}$$

where M_r is the non-relativistic (rest) mass of the vehicle and "a" is the fraction of the original (on-board) propellant mass (non-relativistic) remaining after annihilation (i.e., a=0.22 for the charged pions) to produce forward thrust. Unfortunately, Eq. (4) cannot be integrated analytically. However, if we assume that $V \sim I_{sp}$, such that $(1-I_{sp}V/c^2) \sim (1-V^2/c^2)$, then we obtain an equation:

$$dM_r / M_r = - dV / \{- I_{sp}/c^2V^2+(1-a)V+a\, I_{sp}\} \quad \text{(Eq. 5)}$$

which can be analytically integrated and the integral evaluated for the rocket mass limits of M_o (initial wet non-relativistic [rest] mass) and M_b (final "burnout" dry non-relativistic [rest] mass), and initial and final velocities ($V_i = 0$ and $V_f = \Delta V$), The resulting relativistic Rocket Equation with loss of propellant is:

$$M_o / M_b = \{ [(-2I_{sp}\Delta V/c^2+(1-a)-[(1-a)^2+4aI_{sp}^2/c^2]^{1/2}) (1-a+[(1-a)^2+4aI_{sp}^2/c^2]^{1/2})] / [(-2I_{sp}\Delta V/c^2+(1-a)+[(1-a)^2+4aI_{sp}^2/c^2]^{1/2}) (1-a-[(1-a)^2+4aI_{sp}^2/c^2]^{1/2})] \}^{\{1 / [(1-a)^2+4aI_{sp}^2/c^2]^{1/2}\}} \quad \text{(Eq. 6)}$$

Figure 5 illustrates the values of M_o/M_b calculated by the four versions of the Rocket Equation for an I_{sp} (0.33c) and "a" parameter (0.22) characteristic of a matter-antimatter rocket. In each case, as ΔV becomes large, the relativistic Rocket Equation mass ratio (M_o/M_b) is somewhat larger than its classical counterpart. However, a larger divergence is seen in the effect of loss of propellant mass for thrust (i.e., momentum) production. Thus, the mass ratio M_o/M_b for a relativistic rocket with an I_{sp} of 0.33c requiring a ΔV of 0.25c is around 2.15 if the loss of propellant is ignored; however, if a value of a=0.22 (rather than a=1) is included, the mass ratio more than doubles to about 5.45. We thus have the surprising result that, even with its extraordinarily high I_{sp}, the antimatter rocket is limited to a ΔV per stage of around 0.25c.

This is due to the impact that this large M_o/M_b has on the antimatter rocket's allowable overall propulsion system dry mass. For example, we often define total dry mass (M_b) as the sum of the propulsion system dry mass (M_{dry}) and the "payload" mass ($M_{payload}$), with the payload simply being everything not directly associated with the propulsion system:

$$M_b = M_{dry} + M_{payload} \quad \text{(Eq. 7)}$$

We can also define a propulsion system's overall "tankage factor" (TF) as M_{dry}/M_p; the corresponding TF value for the total stage dry (burnout) mass is thus M_b/M_p. In effect, this ratio sets an upper limit on the propulsion system's tankage factor for the case of no payload. In the case of the relativistic Rocket Equation, the total TF values for M_b/M_p become 0.870 and 0.225 for a=1 and a=0.22, respectively. In practical terms, this means that the maximum allowable tankage fraction for the antimatter rocket is 22.5%; however, the TF of the LH_2 tankage in the Space Shuttle ET is around 25%. Generally, there is some economy of scale in the propellant tankage (i.e., lower TF as M_p increases); nevertheless, we see the need to limit the ΔV delivered per stage so as not to require an impossibly light propellant tankage (and also still have mass left for payload).

Finally, it is worth noting the large flux of gamma rays produced by the annihilation reaction (i.e., almost 38% of the initial propellant rest mass). This tends to drive the overall vehicle geometry to a long and narrow shape, with a single-loop magnet for the magnetic nozzle, so as to minimize the solid angle of intercepted gamma radiation from the annihilation. Nevertheless, as we will see below, there is a need for large radiation shields and an enormous radiator to dump heat from gammas absorbed in the radiation shields.

VEHICLE SUBSYSTEMS

In this section, we will develop the various

scaling equations used to determine the vehicle mass, power, and so on. Figure 6 illustrates the main systems in an antimatter rocket. These systems include the magnetic nozzle, radiation shields (to protect sensitive components from the intense, high-energy gamma ray flux), radiators (primarily to dump heat produced in the shields due to absorbing gammas, as well as waste heat from other spacecraft systems), propellant storage and feed systems, thermal control (insulation and active refrigeration), electric power systems, miscellaneous spacecraft systems (avionics, telecommunications, attitude control, etc.), the payload, and finally a dust shield to protect the vehicle from high-speed impacts with interstellar dust.

High-Temperature (100K) Superconductor Magnet Magnetic Nozzle

The magnetic nozzle consists of a single-loop high-temperature (100K) superconductor coil. This geometry was chosen so as to make use of prior modeling of a similar system in the VISTA (Vehicle for Interplanetary Space Transportation Applications) inertial confinement fusion (ICF) study.[7] A schematic of the magnetic field is shown in Figure 7. The overall geometry has a magnet coil centerline radius (R) that is twice the standoff distance (X) from the ICF implosion or, in our case, the annihilation region. This geometry was also assumed in a Monte-Carlo modeling of the proton-antiproton reaction that was used to determine the "effective" I_{sp} (0.33c) of the antimatter rocket.[8] Sample gamma and charged pion trajectories from the Monte-Carlo analysis are shown in Figure 7. As can be seen, there is imperfect reflection of the charged pions; some of them even travel "upstream" from the annihilation point because of the finite capability of the magnet to turn the ions and direct them "downstream" to produce thrust. Thus, the effective I_{sp} is less than the relativistic velocity (0.94c) of the charged pions.

However, even to achieve this level of performance, a very high magnetic field is required. For example, a field of 138 Tesla is required at the center of the magnet loop (B_o) in order to have a field of 99 Tesla at the annihilation point (B_x).[8] For these analyses, we have assumed a superconducting magnet critical current density (I_o) of $1x10^{10}$ Amps/m^2. For calculating magnet mass, we assumed a material density (ρ) of 5 g/cm^3 (typical of CuO_2-based high-temperature superconductors).

In our calculations, we will use the same geometry where R=2X as has been used previously. Given B_o (or B_x) and X or R, we can calculate the required magnet current (I) from:

$$B_o = \mu_o I / (2 R) \qquad \text{(Eq. 8a)}$$

$$B_x = \mu_o I R^2 / \{ 2 (R^2 + X^2)^{(3/2)} \} \qquad \text{(Eq. 8b)}$$

where μ_o = 1.256E-6 Tesla-m/Amp. The magnet cross-sectional area (A) is then:

$$A = I / I_o \qquad \text{(Eq. 9)}$$

and the magnet mass (M) is:

$$\text{Mass} = \text{Density} \bullet A \bullet 2\pi R \qquad \text{(Eq. 10)}$$

However, we also want to minimize the projected area that the magnet exposes to the intense gamma flux from the annihilation. In order to minimize the exposed area, we assume a rectangular cross-section for the magnet (with a 2:1 aspect ratio) such that the long axis of the rectangle points towards the annihilation point. In this case, "a" is the long axis pointing towards the annihilation point and is twice the transverse axis "b". Also, as discussed below, the gamma ray shield depth (t), which is determined by gamma ray dose and superconductor radiation tolerance, is oriented along the line pointing towards the annihilation point. In addition, we added a nominal shielding thickness (t') on the side of the magnet; (t') was arbitrarily assumed to be 10% of the shield depth (t) so as to account for scattered gammas. Unfortunately, the shield operates at a high temperature (1500 K) to minimize radiator area, so there is a requirement for high temperature multi-layer insulation (MLI) between the 1500K shield and the 100K magnet.

Finally, the intense magnetic field produces a magnet structure hoop stress ($P_{magnetic}$):

$$P_{magnetic} = B_o^2/2\mu_o = 7.6 \text{ GPa (75 kBar)} \qquad \text{(Eq. 11)}$$

To keep the magnet from being blown apart, we assumed a radially surrounding structure of an advanced material like carbon nanotubes or diamond with a yield stress σ_m = 50 GPa, density ρ = 1.9 g/cm^3, and a factor-of-safety SF=2. The required structure thickness (t'') is then:

$$t'' = (R + a/2) * SF * (P_{magnetic} / \sigma_{material}) \qquad \text{(Eq. 12)}$$

Figure 8 illustrates the overall geometry of the various elements (magnet, shield, and structure) in the magnetic nozzle. Finally, note that we have employed a single-loop magnet; earlier studies assumed the use of multiple loops to improve I_{sp} by more efficiently deflecting the charged pions.[9] However, it is not clear if this improved performance would overcome the added radiation shielding and cooling required for multiple magnet loops.

Radiation Shields

A radiation shield is required to protect the superconductors, main radiator, electronics, propellant tanks, payload, etc. from the intense flux of 200 MeV

gamma-rays produced in the annihilation process. We assumed a tungsten shield because of its excellent gamma shielding properties, and because it can be operated at a high temperature (1500K assumed here) to minimize the radiator needed to reject the gamma energy absorbed by the shield. Properties for the shield and representative allowable radiation doses are listed in Tables 3 and 4, respectively.

Table 3. Tungsten Shield Properties for 200 MeV Gammas.

Material	**Tungsten (W)**
Density (g/cm^3)	19.35
Mass Attenuation Coeff. (cm^2/g)	0.097
Attenuation Factor Tau (m)	0005328
Tau = 1 / (Density • Mass Atten. Coeff)	
Reduction in 200 MeV gamma dose per meter of Shield thickness (t) = exp(-t/Tau) =	3.06E-82

NOTE: These calculations do NOT include the effect of scattered gammas. This will result in a need for more shielding.

Table 4. Assumed Allowable Radiation Doses.

Material	**Electronics**	**People**	**Radiator**	**Super-conductor**
Dose (200 MeV Gammas)				
	1E6 rad total	5 rad/ year	1E10 rad total	1.5E6 rad total[10]
Energy Attenuation Coeff. (cm^2/g)				
	0.030	All others assumed same		

The calculation methodology for determining the required shield thickness involves several steps. First, we calculate the total gammas produced by the engine; this will be a function of both total MC^2 power and engine run time. Next, we determine the fraction of the total gammas intercepted per cm^2 of material. This is proportional to 1 / (area of a sphere with radius "r" from the annihilation point). This is one reason why the magnet standoff distance drives vehicle mass and geometry (long and skinny) so strongly. The required shield thickness (t) is then:

$$t = Tau \bullet \ln \{ \text{(Intercepted gammas)} * \text{(Energy per Gamma, 200 MeV)} * \text{(Material Atten. Coeff.)} / \text{(Material Allowed Dose)} \} \quad \text{(Eq. 13)}$$

Finally, the main (1500K) radiator shield is rectangular; the shield volume is its required thickness multiplied by the height of the main radiator (the diameter of the superconductor loop) and the thickness of the radiator. The systems and payload shields are disk-shaped to reflect the cylindrical geometry of the vehicle.

Radiators

There are a number of different types of radiators used by the various systems on the vehicle. The primary (main) radiator is used to reject gamma-ray heat absorbed by the magnet radiation shield. Although it operates at a temperature of 1500K (limited by the radiation shield materials), it is still the dominant radiator that drives the vehicle mass and configuration. However, there are additional smaller radiators for the power system, refrigerators, and payload. Characteristics of the various radiators are summarized in Table 5.

For the smaller radiators, conventional fin-and-tube radiators were assumed. However, for the main (1500K) and electric power system radiators, a more aggressive technology, such as the liquid-drop radiator (LDR), was assumed with a roughly 10-fold reduction in mass per unit radiating area. Also, note that a shield thickness was assumed for the main radiator; this value is used to determine the width of the rectangular radiation shield used to protect the main radiator from gamma radiation. Lastly, the width of the main radiator is fixed by the diameter of the superconductor magnet loop. This results in a very long main radiator (e.g., hundreds of km in length), but it does serve to minimize the radiation and dust shields by keeping the overall vehicle long and thin.

Finally there are some additional subtleties in configuring the various radiators. For example, the main radiator has a simple 2-sided flat plate geometry. By contrast, the power system radiator is assumed to be in a cylinder that only radiates from its outer surface. This configuration was inspired by earlier space nuclear power system studies. A simple flat plate was assumed for the other small systems' radiators because they are relatively small.

Propellant Storage and Feed System

The assumptions for the propellant tankage and feed systems are given in Table 6. The normal-matter hydrogen is stored as ordinary liquid hydrogen (LH_2) and the antimatter as solid anti-H_2 (anti-SH_2). Note that the anti-SH_2 must be stored and fed into the engine using a non-contact magnetic levitation technique. The anti-SH_2 is stored as pellets to allow removal and transport of small quantities of antimatter to engine. For comparison, a 1-mm diameter (4.6 μg mass) anti-SH_2 pellet has an MC^2 annihilation energy equivalent to 2 tons of TNT. However, storage of anti-SH_2 as individual pellets will result in a reduction in its effective storage density. We assumed an effective anti-SH_2 density 1/10 that of liquid H_2 (1/12.57 of solid H_2)

Table 5. Radiator Characteristics.

Radiator for:	Gamma Shield	Cruise Power	Refrigerators	Payload
Temperature (K)				
Hot	1500	600	300	300
Sink	100	200	4	4
Mass/Area (kg/m^2)	0.50	0.50	5.0	5.0
Sample Technology	LDR	LDR	Fin&Tube	Fin&Tube
No. of Sides Radiating	2	1	2	2
Effective Mass/Area (kg/m^2)	0.25	0.50	2.5	2.5
Emissivity	0.9	0.9	0.9	0.9
Effective Mass/W_t ($kg/kW_{thermal}$)	0.00097	0.07655	6.048	6.048
Radiator Thickness (m)	0.125	0.125	0.020	0.020

The tank mass is calculated on the assumption of a cylindrical tank (whose diameter is fixed by the superconductor magnet diameter) with hemispherical end-domes. The required tank size is first found based on the volume of propellant required plus any tank ullage (i.e., the volume of vapor above the liquid). With the tank dimensions known, the tank mass is calculated using a tank wall thickness of 0.5 mm (19.7 mil). For comparison, the Centaur LO_2/LH_2 chemical stage has tank walls of 10 mil; a soda pop can has a wall thickness of 3 mil. We assumed that a minimal tank pressure (e.g., 30 psia LH_2) would allow the use of thin tank walls. However, it may be necessary to substantially increase the wall thickness if the propellant tanks are used as vehicle structure.

Table 6. Propellant Tank Properties.
(Cylindrical tanks with hemispherical end-domes)

Propellant	LH2	Anti-SH2 (Pellets)
Density (g/cc)	0.070	0.007
Tank Material	Al	
Wall Thickness	0.5 mm (19.7 mil)	
Ullage	5% Mp	(None)
Miscl. Structure, Feed, etc.	1% Mp	2% Mp
Losses, Boiloff	1% Mp	5% Mp

M_p = Useable (i.e., ΔV) propellant mass.

Note that the sizing of the propellant feed systems represents a completely arbitrary assumption; this is an area that will need much more study to evaluate options and determine their mass and power requirements. For example, we have identified two options for consideration in future studies. In the first, the anti-SH_2 pellets are fed magnetically down a long tube (100s of km in length at 1K next to a 1500K radiator!) in to the engine. A second option would be to first convert the anti-SH_2 into antiprotons, and feed the antiproton ions down to the engine in what is basically a particle beam. This option was assumed in this study.

To do this, the solid must be vaporized, ionized, and the ions accelerated to some significant speed in the particle beam. This requires electrical energy that would be supplied by the electric power system. For these calculations, we assumed a particle beam ion (antiproton) velocity of 0.1%c, which gives an energy requirement of 4.65×10^{10} J/kg. Combining this with an assumed electrical efficiency of 90% and a propellant mass flow rate gives the electric power requirement. Note however that one disadvantage of this approach is that the ion space-charge limit would result in the requirement of a very large diameter beam tube because of the large propellant flow rate needed. For example, with a space charge limit of 10^{10} ions/cm^3, the tube diameter would be almost three times larger than the diameter of the 4th stage of the nominal vehicle described below. However, this effect was ignored in these analyses.

Thermal Control (Insulation and Refrigerators)

Insulation and active cooling are typically needed for low-temperature components like the magnets and propellant tanks. Tables 7 and 8 list the sizing assumptions for these systems.

Table 7. Insulation Characteristics.

Application	Magnet	LH_2 Tank	Anti-SH_2 Tank
Temperature (K)	100	20	1
T_{sink} (K)	1500 (Hot Shield	4 (Space)	4 (Space)
Type	20 Layer-Ti/Kapton MLI	MLI	MLI
Insulation Areal Density (kg/m^2)	10.5	1.0	1.0
Four Conical Thermal Shields (at Ends of Tanks) and Structure Supports (Connecting Tanks to Rest of Vehicle, Penetrate MLI): Mass (kg) per m^2 of Tank Cross-Section Area	- - -	0.629	0.629
Heat Soak (W_{cool}/m^2 of Surface)	544	0.00	2.00E-05
Heat Soak Contingency (%)	0%	0%	10%
Heat Soak (W_{cool}/m^2) Used in Calculations	544	0.00	2.20E-05

Three different types of refrigerators were sized. The first operates at 100 K to provide active

cooling for the superconductor magnet, the second at 20 K for normal-matter liquid-H_2, and the third at 1K for solid anti-H_2. Characteristics of the three refrigerators are summarized in Table 8. Surprisingly, a LH_2 refrigerator (20K) was not required because the LH_2 tank could passively radiate to the 4K thermal sink of deep space. Also, although the anti-SH_2 refrigerator is mass- and power-intensive, the cooling load on the SH_2 tank is modest (see below), so that the 1K refrigerator is not a strong system mass driver. However, because the superconductor magnet is next to a 1500K heat source (its radiation shield), the magnet refrigerator does represent a significant element in the magnetic nozzle system.

Table 8. Refrigerator Characteristics.

Application	**Magnet**	**LH_2 Tank**	**Anti-SH_2 Tank**
Temperature (K)	100	20	1
Type	Stirling	Sorption	Sorption
P_e (W_e) per W_{cool}	10	200	10,000
Mass (kg) per W_{cool}	10	100	1,000
Radiator Type	Fin&Tube	Fin&Tube	Fin&Tube
2-Sided Radiator Area (m^2) per W_{cool}	0.013	0.243	12.098

Finally, note that the thermal loads calculated above assume that the vehicle is edge-on to any nearby heat sources, such as a star or planet. This implies that the antimatter rocket is a true deep space vehicle. Thus, a separate propulsion system will probably be needed for transporting the payload around the target solar system. One plausible candidate would be a Nuclear Electric Propulsion (NEP) system; the vehicle already has a dedicated electric power system that could be combined with an electric propulsion system to provide the relatively small (at least as compared to 0.5c) ΔV needed for operations within a solar system. Alternatively, additional refrigeration capacity could be added to allow the antimatter rocket to operate safely within the warm environs of a solar system.

Electric Power System

An electric power system is needed to supply power for operating the antimatter rocket engine, refrigerators, propellant feed system, and so on. The system was sized as a simple two-parameter curve fit of specific mass (kg/kW_e) values typically seen for NEP vehicles. This results in an equation of the form:

$$\text{Specific Mass } (\alpha, kg/kW_e) = A * (P_e, MW_e)^B \quad \text{(Eq. 14)}$$

where: A = -0.5
B = 15.80.

The system mass is simply:

$$\text{Mass (MT)} = (\text{Specific Mass, } kg/kW_e = MT/MW_e) * (\text{Power, } MW_e) \quad \text{(Eq. 15)}$$

Note however that this can result in an unrealistically low specific mass and corresponding system mass when extrapolated to the high powers found in the antimatter rocket systems. For example, as shown in Figure 9, the power system's specific mass falls below the intrinsic specific mass of the power system's radiator at sufficiently high power levels. Thus, in our calculations, we have limited the minimum power system specific mass to that of its radiator. (The radiator specific mass is based on an assumed thermal-to-electric conversion efficiency of 30%.)

Finally, the total electric power is the sum of the power needs of the Payload (10 MWe), Miscellaneous Systems (10 MWe), Refrigerators (dependant on the cooling load), Engine (assumed to be 10^{-6} of the total engine MC^2 power), and propellant Feed System (dominated by the power needed to accelerate the antiprotons to 0.1%c).

Spacecraft Miscellaneous Systems

An allocation of 100 MT was made to account for the various miscellaneous spacecraft systems like avionics, telecommunications, attitude control, etc. We also assumed an arbitrary total requirement of 10 MW_e electric power for these systems.

Payload

A robotic payload was assumed with a mass of 100 MT and an electric power requirement of 10 MW_e. However, as will be seen below, the mass of the payload is insignificant compared to the other vehicle systems.

Dust Shield

A cylindrical dust shield is placed at the front of the vehicle to protect it from relativistic dust impacts. As shown below, the shield thickness is a function of the vehicle velocity, the distance traveled, and the number of hydrogen atoms per unit volume (H/cm^3) in interstellar space. The calculation methodology used here assumes that the kinetic energy of the dust impacts is turned into thermal energy that evaporates (sublimes) the shield material (graphite). Thus, it is necessary to take into account the energy per unit mass of dust at a given velocity, and then determine the total mass of dust hitting the shield.

The numerical distribution of dust particle sizes, and thus masses, is known from astronomical observations.[11] This is found by measuring the light from a known source; just as in the Earth's atmosphere, dust causes a reddening of the observed light. From this

data, a particle number and size (radius) distribution can be deduced:

$$dN = A * N(H) * R^{B} * dR \qquad \text{(Eq. 16)}$$

where

N = Number of particles per cm^3 of space in the size range R to R+dR
A = 7.94E-26 $cm^{2.5}$ / (#H atoms)
N(H) = #H atoms/cm^3 (Assumed = 1.00 H / cm^3)
R = Particle Radius (cm)
B = -3.5 (Exponent on R)
R_{min} (microns) = 0.005 (Integration Limits)
R_{max} (microns) = 0.25

This can be used to determine the particle mass distribution by using the relationship between mass, density (ρ), and radius:

$$dm = \rho * 4/3\pi R^{3} \qquad \text{(Eq. 17)}$$

$$\begin{aligned} dM &= dm * dN \\ &= [\rho * 4/3\pi R^{3}] * [A * N(H) * R^{B} * dR] \\ &= \rho * 4/3\pi * A * N(H) * R^{(B+3)} * dR \end{aligned} \qquad \text{(Eq. 18)}$$

This can be integrated and evaluated at the limits of R_{min} and R_{max}:

$$M = \rho * 4/3\ \pi * A * N(H) * R^{(B+4)} / (B+4)\ ]_{Rmin}^{Rmax} \qquad \text{(Eq. 19)}$$

The final numerical value (for an assumed ρ = 2.65 g/cm^3 representative of a silicate dust particle) is 7.570E-27 grams of dust per cm^3 of space. Finally, this value is multiplied by the distance traveled to give a total mass hitting the shield per unit area of shield (i.e., grams/cm^2 of shield area).

We then use the peak velocity of each stage (e.g., 0.25c for stage 1 and 0.5c for all other stages) to determine the (relativistic) impact energy per unit mass, and multiply this by the mass of particles hitting the shield. Finally, this gives us a total energy absorbed by the shield per unit area of shield.

We next take the kinetic energy (KE = 1/2 MV^2 times the Relativistic Mass Correction) of the dust particle impact and assume that this causes the dust shield (graphite) to evaporate (sublime) such that the shield mass lost is ($KE/\Delta H_{sub}$), with ΔH_{sub} for graphite = 59,866 J/g. This then gives us the shield mass loss (per cm^2 of shield frontal area); dividing by the density of graphite (2.25 g/cm^3) gives the required shield thickness with the shield diameter that of the superconductor magnet.

To add margin to the shield mass, we assumed arbitrarily that additional shield material would be "spalled" (mechanically broken) off of the surface by the shock of impact such that the total shield material lost would be ten times that calculated based on ($KE/\Delta H_{sub}$). We further assumed a 50% margin on the required diameter and a final 50% mass margin. However, because "lower" stages are partly covered by "upper" stages, a hole with the diameter of the next upper stage is subtracted from the shield. Finally, as with the magnet, we see how a need to minimize the size (diameter) of the Dust Shield drives the overall vehicle geometry (e.g., long and skinny).

One final observation is that an interstellar rendezvous vehicle is only at high speed in interstellar space. By contrast, flyby mission vehicles encounter thick solar system dust clouds at high speed. Thus, we have the somewhat paradoxical situation that the dust shield for an interstellar flyby could be larger (heavier) than the one needed for a rendezvous mission.

System Mass Contingency

An overall mass contingency of 30% of the vehicle dry mass (but not payload) was included. The 30% value is typical of mission design studies and is intended to reflect the sort of mass growth seen over a spacecraft's design life. Basically, it represents everything else we forgot to include. Note however that this may be an inappropriate estimate based on the fact that we are trying to size a vehicle that may be a century in the future; there may be significant technology improvements that could make this an overly conservative estimate. Nevertheless, this must be tempered with the realization that there is also the potential for significant mass growth from systems that have not been treated in detail, such as structure or the antimatter storage and feed system.

VEHICLE SIZING

With the various scaling equations described above, it is possible to evaluate the "dry" and "wet' mass of the vehicle. For calculation purposes, we will assume a mission to 40 LY with a cruise velocity of 0.5c, so that a 4-stage vehicle is required (i.e., two to accelerate up to 0.5c and two to decelerate to a stop.

Calculation Methodology

We implemented the various scaling equations in Microsoft® Excel; alternatively, the calculations could be performed using a computer program. In either case, it is important to use an iterative technique (e.g., the Iteration option enabled in Excel) because of the complex interaction between the various systems.

We used the Magnet Coil standoff distance (X=R/2) as the free parameter in the calculations, with the magnetic field strength (B_o, B_x) fixed. From this

starting point, it is then possible to calculate the required magnet current, cross-sectional area (given I_o), mass, and so on. The overall vehicle dry and wet mass is calculated (iteratively) at each X. We then determine the optimum X (and thus R) that gives a minimum total dry (and wet) mass.

There are several practical considerations in performing these calculations. For example, as shown in Figure 10, the vehicle dry mass "blows up" at low values of X, so that it is necessary to add a mass cutoff term, e.g., in Excel, a calculation like =IF(mass>1e6,1e6,mass), to prevent wasting calculations or even numerical overflow. There is also a very significant "ripple effect" for a multi-stage vehicle, because wet Stage "N" is payload for Stage "N-1." This has the effect of making the lower stages really big; thus there is a needed to hand-tune the initial (minimum) magnet standoff distance (X) and X step size (ΔX) for each vehicle stage so as to avoid wasted calculations, and to ensure that a large enough range of X values is covered to identify the optimum (minimum mass) X.

Calculation Results

Results of the calculations are shown in Figures 10 and 11. All the calculations are shown for a mission with a cruise velocity of 0.5c and a distance of 40 LY. (This distance is only significant in determining dust shield mass.) Generally, components like the magnet (and its associated insulation, structure, and refrigerator), radiation shields, power system, miscellaneous systems, and dust shield are a relatively small fraction of the total dry mass. Not surprisingly, the main (1500K) radiator, propellant tanks (and their associated feed system, insulation, and refrigeration), and overall dry mass contingency (30%) represent the major dry mass components of the vehicle.

System Mass Variation with Magnet Coil Radius. Figure 10 illustrates the interaction between the various systems as a function of magnet coil radius (R=2X). For example, the radiation shields and magnet components increase monotonically with increasing magnet radius. However, at small values of X and R, the radiation shields intercept a larger fraction of the gamma radiation power, so the radiator mass "blows up" at small R. This in turn increases tankage and contingency mass at small R. Also, because of the increased mass, the engine jet power increases (to maintain a T/W of 0.01 gee), so the electric power system mass increases.

Gradually, as R increases towards the minimum-mass (optimum R) point, less radiation power is intercepted by the shields, so there is a decrease in the mass of several of the systems. However, past the minimum-mass point, the increase in the physical size of the magnet begins to impact the shield size. This again results in an increase in the fraction of the intercepted gamma power, and again the radiator mass begins to grow. Added to this is the increased mass of the larger-radius magnet and dust shield, such that the overall vehicle dry mass begins to increase as large values of R are encountered.

Comparison of 4-Stage Vehicle Systems. Figure 11 shows a comparison for each of the stages of a 4-stage vehicle. Because of the large value of the Rocket Equation mass ratio (M_o/M_b=5.45) for each stage, there is an enormous increase in mass and power as we go from the "top" (last) 4th stage to the "bottom" 1st stage. Even if we had a propulsion system with no dry mass, the 1st stage would still have a mass of 5.45^4=882 times the 4th stage's payload mass. Thus, the antimatter propellant requirement is an almost unbelievable 200 million metric tons, larger even than the mass of the Three Gorges Dam in China. Similarly, the engine jet power is comparable to all the sunlight hitting Earth; even the electric power required just to operate the engine rivals the total power output (of all kinds) of Human Civilization (ca. 14 TW).

Needless to say, these are not near-term capabilities. Nevertheless, they do more than adequately satisfy our intension of creating a stretch goal which taxes out technological capabilities. However, it again must be stressed that any interstellar mission will require enormous resources; the simple act of a 1-MT spacecraft (roughly of the dry mass of a typical robotic spacecraft) traveling at 0.5c represents a kinetic energy content of about 20 day's worth of the total energy produced by Human Civilization (ca. $2x10^{20}$ Joules per year).

Finally, it is worth noting that the results obtained above are a function of the systems assumptions that we have made. Generally, we have been relatively conservative in using values (parameters) to describe the various systems. Thus, these results can be considered a "worst case" in that future technological improvements can result in dramatic reductions in vehicle mass. In the next section, we will investigate the impacts that different (e.g., more optimistic) parameter assumptions could have on overall vehicle performance.

PARAMETRIC EVALUATION OF SYSTEMS SENSITIVIES

In this section, we vary the system performance parameters (e.g., critical current, efficiency, specific mass, etc.) of the various systems to evaluate impact of potential performance improvements. For example, how does a 10-fold improvement above the nominal technology parameter assumption improve performance (e.g., dry mass) of the vehicle? This type of a parametric analysis has several advantages. First, it identifies high-leverage

technologies (e.g., those technologies where a 10-fold improvement produces a large drop in mass). As a specific example, shown in Figure 12, if we increase the magnet critical current density (I_o) by a factor of 10, the 4th stage dry mass drops to only 44% of its dry mass for the nominal parameter value (37% of nominal-value mass for the total 4-stage vehicle). Note also that because of the strong interaction between systems, a smaller magnet will in turn result in a smaller magnet structure, radiation shield, shield radiator, magnet refrigerator, refrigerator power, and so on.

A parametric analysis also helps identify low-leverage technologies where performance is already good enough (i.e., there is modest or negligible drop in mass for a 10-fold improvement in the technology). Ultimately, this allows us to prioritize our technology investment strategy so as to focus on the high-leverage technologies that yield the greatest benefit.

Finally, this analysis helps identify the sensitivities of arbitrary assumptions. For example, what if our assumed value is 10 times worse (or better) than the assumed nominal value. Parameters such as the assumed engine electric power (e.g., 10^{-6} of engine MC^2 power) that were arbitrarily assumed could in fact badly skew the results if they have a major impact on mass.

Parametric Sensitivities

Results of the parametric analyses are given in Tables 9 and 10. In the context of these parametric analyses, it is important to remember that some problems can't be fixed with technology. For example, the basic physics inherent in matter-antimatter annihilation physics means that we will always have only 22% of the initial p+/p- mass as charged pion rocket exhaust mass, with the resultant doubling of M_o/M_b as compared to that of a rocket without propellant loss. On the other hand, some problems can be attacked with improved technology, like improved magnet critical current (I_c), radiator mass, and so on.

High-Leverage Technologies. From Table 9, we see that several system technology improvements can have a significant impact on the overall mass of the vehicle. For comparison purposes, we assumed a 10-fold improvement in a given technology parameter and compared the resulting vehicle mass to the nominal-values 4th stage of the 0.5c cruise, 40 LY vehicle. The high-leverage technologies include the main (1500 K) radiator (vehicle mass only 26% of the nominal 4th stage), the anti-SH_2 effective density (30% of nominal), the magnet critical current density (44% of nominal), the propellant tank mass (52% of nominal), the anti-SH_2 "boiloff" (annihilation with walls, etc.) losses (54% of nominal), and the magnet refrigerator mass (71% of nominal) The other technologies have negligible or small impacts on overall vehicle mass.

Several of these systems are likely candidates for improvement independent of their use on an antimatter rocket, such as radiators and superconducting magnets. Similarly, improvements in vehicle structures (e.g., tanks, etc.) and active refrigeration systems are cross-cutting technologies applicable to a variety of space applications. However, some areas, specifically those dealing with anti-SH_2 storage and feed, are unique to the antimatter rocket application (although they could become more generally important if antimatter were used as commonly as, for example, LH_2 or even fossil fuels are used today). However, recognize that there may be some inherent physical limitations in improving some of these areas; for example, increasing the effective storage density of anti-SH_2 10-fold has a significant benefit, but this effective density would be comparable to that of LH_2 (e.g., 0.07 g/cm^3).

Sensitivity of Arbitrary System Parameter Assumptions. One significant concern is the impact that arbitrary assumptions can have on overall vehicle sizing. As mentioned previously, engine electric power was arbitrarily assumed to be 10^{-6} of engine MC^2 power. Making this value 10 times worse (i.e., 10^{-5}) almost doubles (1.81 times larger) the mass of the 4th stage. This strongly suggests the need for detailed system modeling of the thruster system's electric power requirements. An even more sensitive set of assumptions are those associated with the dust shield. For example, assuming a 10-fold increase (worsening) in either the interstellar hydrogen density (and thus dust density) or the spalling factor (numerically the effect is the same for either one) results in a 4th stage 6.31 times heavier than the nominal case. By contrast, a 10-fold improvement decreases the 4th stage mass to 52% of the nominal. This suggests that an important goal of remote-sensing and/or precursor missions is collection of data that could be used to map out the distribution of interstellar dust. Equally important is an improved understanding of relativistic dust impacts on candidate dust shield.

Payload Mass Assumptions. In our analyses, we have assumed a 100 MT payload mass as an estimate of a very large robotic payload with numerous landers, probes, remote-sensing telescopes, chemical/ biological analytical laboratories, and so on. One question that arises is that of the potential benefits of using micro-technologies to dramatically reduce the payload mass. However, as shown in Table 10, there is a negligible drop in mass for using a 10-fold smaller payload (e.g., 10 MT), so while micro-technology components may be desirable, they are not a driver for this mission. In part, this is because the overall stage mass is driven so strongly by magnet standoff distance (X) and not by payload mass. Also, even at the nominal 100 MT, the payload mass is already a small fraction of the total dry mass of the stage.

We see this even more clearly when we consider heavier payloads. For example, a 10-fold increase in payload mass (1,000 MT) only produces a 4% growth in 4th stage mass. Even for a payload that might be considered for a multi-generation human mission (e.g., 1,000,000 MT, comparable to 1/10th of an L5 Space Colony) only increases the mass of the total nominal 4-stage vehicle by a factor of 18. Thus, payload mass is not a major driver in sizing the vehicle.

Table 9. Antimatter Rocket Parametric Scaling. (Stage 4, ΔV=0.25c, 40 LY)

Quantity	**Baseline Value**	**Parametric Scaling Eq. (Baseline N=1)**	**Wet Mass (for N=10) Wet Mass (for N=1) (%)**
Magnet Critical Current, I_o (A/m^2)	1.0E+10	Baseline * N	44.37%
Magnet Structure			
Tensile Strength, σ (GPa)	50	Baseline * (N=5)	98.46%
Density (g/cm^3)	1.9	3.5 (Diamond)	101.61%
Radiator Emissivity, ε	0.90	Fixed	
Refrigerator Electric Power (W_e /W_{cool})			
100 K (Magnet)	10	Baseline / N	Negligible Change
20 K (LH_2 Tank)	200	Baseline / N	Negligible Change
1 K (Anti-SH_2 Tank)	10,000	Baseline / N	Negligible Change
Refrigerator Mass (kg/W_{cool})			
100 K (Magnet)	10	Baseline / N	71.04%
20 K (LH_2 Tank)	100	Baseline / N	Negligible Change
1 K (Anti-SH_2 Tank)	1,000	Baseline / N	99.16%
LH2 Propellant Tank			
Wall Thickness, t_w (mm)	0.50	Baseline / N	52.20%
Liquid Ullage (% M_p)	5%	Baseline / N	99.57%
Miscl Structure, Feed, Pressurant, etc. (% M_p)	1%	Baseline / N	88.36%
Losses, Boiloff (% M_p)	1%	Baseline / N	88.28%
Anti-SH2 Propellant Tank			
Wall Thickness, t_w (mm)	0.50	Baseline / N	Combined w/ LH_2
Solid Ullage (% M_p)	0%	Fixed	
Miscl Structure, Feed, Pressurant, etc. (% M_p)	2%	Baseline / N	78.02%
Losses, Boiloff (% M_p)	5%	Baseline / N	54.41%
Effective Anti-SH_2 Density (g/cc)	0.0070	Baseline * N	30.47%
Dust Shield			
N(H) (#H atoms/cc)	1.0	Baseline / N	49.11%
10X Baseline Example	*1.0*	*Baseline * N*	*630.58%*
Spalling Factor, F	10	Baseline / N	49.11%
Thickness Contingency	50%	Baseline / N	82.86%
Radius Contingency	50%	Baseline / N	71.09%
Cruise Electric Power System			
Specific Mass (α) = A*Pe^B	A=15.80	Baseline / N	Negligible Change
	B=–0.50	Fixed	
Efficiency (Thermal->Electric)	30%	Fixed	
Engine Miscl Electric Power			
Fraction of Total MC^2 Power	1.0E-06	Baseline / N	96.66%
10X Baseline Example	*1.0E-06*	*Baseline * N*	*180.70%*
Engine Anti-Proton Feed System Electric Power Calculations			
Ion Space-Charge Limit (Ions/cc)	1.0E+10	Baseline * N	Negligible Change
Ion Velocity (%c)	0.1%	Fixed	
System Efficiency	90%	Fixed	
General Contingency	30%	Baseline / N	35.87%
Miscl Systems			
Mass (MT)	100	Baseline / N	99.19%
Power (MW_e)	10	Baseline / N	Negligible Change
Radiator Mass (kg/$W_{thermal}$)			
Gamma Shield (2-Sided Flat Plate)	9.677E-07	Baseline / N	26.43%
Cruise Power (1-Sided Cylinder)	7.655E-05	Baseline / N	Negligible Change
Allowable Radiation Doses	(all fixed for given material type)		

Table 10. Antimatter Rocket Payload Parametric Scaling. (ΔV=0.25c per Stage, 40 LY)

Quantity	Baseline Value	Parametric Scaling Eq. (Baseline N=1)	Parametric Value	Wet Mass (for Given Value) / Baseline Wet Mass (for N=1) for Total 4-Stage Vehicle	
				Nominal Vehicle	10X Better Rad & Mag Vehicle
Payload Power (MW_e)	10	Baseline / N=10	1	0.9998	0.9995
		Baseline * N=10	100	1.0020	1.0051
Payload Mass (MT)	100	Baseline / N=100	1	0.9950	0.9824
		Baseline / N=10	10	0.9954	0.9841
		Baseline * N=10	1,000	1.0441	1.1480
		Baseline * N=100	10,000	1.4130	2.2242
		Baseline * N=1,000	100,000	3.7095	9.1288
		Baseline * N=10,000	1,000,000	17.8044	59.3306
		Baseline * N=100,000	10,000,000	120.1306	483.1776

Acceleration Assumptions. For our nominal system, we assumed an acceleration (T/W) of 0.01 gees for each stage. This has a significant impact on trip time; for example, for a 40 LY rendezvous mission, the trip time is 128.5 years with an acceleration (and deceleration) of 0.01 gees and a cruise velocity of 0.5c. This can be compared to the ideal limit of "infinite" acceleration, with no time spent in the acceleration or deceleration phase, where the trip time is simply the distance divided by cruise velocity, or 80 years for a 40 LY trip at 0.5c. For our nominal vehicle, if we increase the acceleration to 0.02 gees to reduce the trip time to 40 LY to 104 years, the vehicle mass is 4.63 times heavier than the 0.01 gee case. The situation becomes even worse as we go to higher acceleration; for example, at 0.3 gees (96 year trip to 40 LY), the vehicle has grown to 16.3 times the mass of the nominal (0.01 gee) case. As discussed previously, this rapid growth in mass is due to the interrelationship between thrust, weight (mass), power, and I_{sp}.

Potential for Synergistic System Improvements

Because of the interactions between the various system elements, there is a potential for significant synergistic dry mass reductions that could be enabled by improvements in only a small number of system parameters. As an example, we will consider 10-fold improvements in the superconductor critical current density (I_o) and the main (1500 K) radiator areal mass (kg/m^2). We chose these two as being likely candidates for technology advancement independent of their use on an antimatter rocket. As shown in Figures 13 and 14, this produces a reduction in the 4th stage mass to only 23% of its nominal value (18% of the total 4-stage nominal vehicle). Thus, instead of requiring almost 200 million MT of antimatter, we need "only" 39.3 million MT; the total vehicle is reduced to a wet mass of 80.7 million MT (roughly the mass of Three Gorges Dam), and a first stage engine jet power of 122,650 TW. Although these values for the vehicle are still enormous, they do illustrate the potential for dramatic reductions in system mass and power that can be realized by improvements in just a few key systems.

Trading Acceleration, Cruise Velocity, and Vehicle Mass

Another interesting potential benefit of this approach is the possibility of allowing higher accelerations without such a severe mass impact as for the nominal systems. For example, Table 11 and Figure 14 illustrate the potential tradeoffs between acceleration (T/W), cruise velocity (V_{cruise}) and thus ΔV per stage, and system parameter assumptions (for the nominal and 10X better radiator and magnet vehicle cases).

For the nominal vehicle with a cruise velocity of 0.5c (ΔV=0.25c per stage), increasing acceleration from 0.01 to 0.03 gees results in a 16.3-fold growth in total vehicle mass. However, reducing the cruise velocity to 0.35c brings the total vehicle mass back to the nominal case (because of the reduction in the Rocket Equation mass ratio M_o/M_b with reduced ΔV per stage), although the reduction in cruise velocity essentially eliminates the trip time benefits of higher acceleration (e.g., only a 2.5 year reduction in trip time from the nominal-case 128.5).

However, the mass reductions inherent in the 10X better radiator and magnet vehicle dramatically reduce the impact of higher acceleration. In this case, going from 0.01 to 0.03 gees (with a cruise velocity of 0.5c) only causes the total vehicle to grow by a factor of 1.53, but the trip time drops from 128.5 to 96.2 years. Furthermore, if we reduce the cruise velocity only slightly to 0.48c, the 0.03 gee vehicle has the same mass as its 0.01 gee, 0.5c counterpart, but with a trip time of 99.2 years. Thus, there is a potential to investigate an interesting trade space of acceleration, cruise velocity, and system mass (parameters) assumptions so as to identify an optimum minimum mass and trip time case.

Table 11. Tradeoffs in Acceleration, Cruise Velocity, and Trip Time for the Nominal and 10X Better Radiator and Magnet Vehicle.

Acceleration	Nominal Vehicle	10X Better Rad&Mag Vehicle
a=0.01gees	$1.00M_o$ V_c=0.5c TT=128.5 yr	$0.18M_o$ V_c=0.5c TT=128.5 yr
a=0.03gees	$16.32M_o$ V_c=0.5c TT=96.2 yr	$0.27M_o$ V_c=0.5c TT=96.2 yr ($1.53M_o$ of 10X Better)
a=0.03gees	$1.00M_o$ V_c=0.3488c TT=126.0 yr	$0.18M_o$ V_c=0.4774c TT=99.2 yr ($1.00M_o$ of 10X Better)

DISCUSSION

A number of additional areas have been suggested by the analyses presented above. First, there is considerable additional work needed to fully develop the antimatter rocket concept. This includes both modeling and experiments. There are also additional technologies common to any interstellar propulsion system that will require development. Interestingly, the general subject of antimatter propulsion and interstellar missions has the potential for significant public outreach, education, and science. Finally, given the enormous scale of the antimatter rocket, it is not unreasonable to consider the fraction of total resources that a civilization would divert for an interstellar mission.

Additional Modeling/Experimental Work Needed

In this study, several components were estimated only as somewhat arbitrary assumptions. These included the propellant storage and feed system, the electric power system, structure, dust shield erosion/spalling, miscellaneous spacecraft systems, and the payload. As discussed above, these assumptions have been treated parametrically to see the sensitivity of the assumptions; however, any improved estimate of the mass, power, etc. for these subsystems will need first-principles modeling and/or analyses that were beyond the scope of this study. In addition to the systems modeling activities described above, there is also a need for improved experimental or computational data in several areas. For example, we need better values for proton-antiproton annihilation product distribution, gamma scattering off of the radiation shield, and, ultimately, demonstration of improved techniques for production and storage of antimatter.

Propellant Storage and Feed System. The propellant storage and feed system (tankage, antimatter levitation and feed system) needs a better understanding of its mass and electric power requirements. This would include the antimatter storage system magnets, the feed system levitation lasers or magnets, and so on. This would also include determination of the insulation and cooling requirements for the feed lines. More generally, a trade should be performed to assess if it is better to feed the antimatter as solid-H_2 pellets, or as an ion beam of antiprotons (the method assumed here).

Electric Power System. For the electric power system, one major need is for a realistic estimate of the electric power required to run the vehicle, and the electric power system mass. For example, what does it really take to run the engine's superconductor magnet, the antimatter storage and feed system, etc. Also, even with a realistic power estimate, we shouldn't arbitrarily scale near-term MW_e NEP-type power systems to TW_e power levels. Instead, it would be more appropriate to determine the characteristics of a very advanced, ultra-high power space nuclear-electric power system where, for example, a fusion power system might be more appropriate in this power regime than fission.

Structure. Another area requiring additional analysis is the vehicle structure. Currently, this is arbitrarily included in the 30% contingency. We need realistic structure requirements, options, and masses, especially given the unique geometry of the vehicle. For example, it might be possible to use the propellant tanks act as structure, although the acceleration loads might cause longitudinal buckling. (This was one reason to use moderately thick-walled tanks as compared to existing aerospace applications.) Also, there will probably be a need for active structures control because of the vehicle's length (to prevent wagging or flexing); thus, it may be necessary to determine the mass and power for an active structures control system. Finally, note that the structural requirements for an antimatter rocket may be non-trivial; for example, the 1st stage antimatter rocket engine thrust (for the 10x better radiator and magnet vehicle) is 552 M-lb_f, equivalent to the total thrust from 74 Apollo-Saturn V launch vehicles at liftoff.

Dust Shield Erosion/Spalling. Dust shield erosion/spalling is another area that had to be arbitrarily assumed. Is there any prior work relevant to 0.5c impacts? More generally, how would you model or test dust impacts at 0.5c? This issue also leads to an intriguing possibility: given the requirement to test micron-sized dust impacts at 0.5c, could we, in an era of interstellar missions, develop the technologies required to accelerate microbe-sized micro- (nano-? femto-?) spacecraft to 0.5c for interstellar flybys? (Interestingly, there are biological examples of light-sensing organelles in microorganisms that could serve as models for "cameras" in ultra-micro spacecraft.) Finally, in our analyses, we assumed that the dust shield

was placed at the front of the vehicle; however, during deceleration, the back (magnet) end points forward. Thus, during the deceleration phase, is a dust shield needed for the thruster magnet (and radiator, tanks, etc.), or will the engine "exhaust" vaporize or deflect interstellar dust before it hits vehicle?

Miscellaneous Spacecraft Systems and Payload. Another area requiring further definition is the Miscellaneous Spacecraft Systems and Payload. For example, what are realistic mass and power for these systems? Also, we have not included any attitude control for the vehicle; we assumed that small (e.g., negligible) auxiliary magnets could be used to slightly deflect the charged pion stream to provide vehicle pitch and yaw during engine operation. However, this does not take into account roll control, or general attitude control while the main engine is not operation. (There is, ironically, the potential requirement that an antimatter rocket might require something as mundane as hydrazine attitude control thrusters.) Finally, it would be desirable to determine a Payload strawman science package with orbiters, landers, etc.

Proton-Antiproton Annihilation Product Distribution. We need better values for proton-antiproton annihilation product distribution (e.g., number of $\pi^{+/-}$, π^{o}) because different numbers are quoted by different authors.[12] This is an important piece of data because of the strong impact that "a" has on the relativistic antimatter Rocket Equation. Also, because of the relatively low value of “a” in a normal proton-antiproton annihilation, we would recommend investigation of innovative matter-antimatter annihilation reactions that might increase the number of charged products (i.e., increase "a").

Gamma Ray Scattering. For the gamma ray shielding, it would be desirable to include the effect of scattered gammas by performing a Monte-Carlo calculation of the shielding. Also, although not treated by our analyses, shielding may be needed for the antimatter feed system, the main magnet structure, or other structure near the annihilation point.

Production and Storage of Antimatter. One very important long-term consideration is the production and storage of enormous amounts of antimatter. This will require research into innovative antiproton production technologies because, just by itself, this is a potential major show-stopper. Ultimately, to perform our “Vision” mission, we will need tens of millions of MT of antimatter produced at near-ideal efficiency (ca. 0.01%);[4] by contrast, today we make tens of ng at 10^{-9} efficiency. Some experimental work in this area has already been done under SBIR (Small Business Innovative Research) and NIAC (NASA Institute for Advanced Concepts) funding.

A related issue is the conversion of antiprotons (and positrons) into anti-H, then into anti-H_2 and finally into anti-SH_2 ice. Again, this is a potential major show-stopper; as with antiproton production, we will need a “non-contact” process capable of high throughput and high efficiency. Some of the required steps have been demonstrated for antimatter but at low rates and efficiencies (e.g., production of thousands of anti-H), and some steps have been demonstrated for normal matter using "non-contact" techniques (e.g., laser cooling). We recommend research programs to demonstrate all the required steps. Initially, this can be done using normal-matter with non-contact technologies (to emulate eventual use with antimatter). An important part of this experimental program would be the demonstration of scalability to high throughput and high efficiency. Finally, we would recommend improved measurements of solid H_2 properties (especially sublimation vapor pressure) at very low temperatures (e.g., < 4 K).

Technologies Common to Any Interstellar Mission

Although the focus of this paper has been on antimatter propulsion technology, there are several additional critical technologies that will require major advancements. For example, because of the finite limit of the speed of light, round-trip communication times will be measured in decades. Thus, the vehicle will require extremely advanced autonomy (e.g., software) and avionics (e.g., hardware) (separate functions in today's spacecraft) that will grow to become a single function. Similarly, structures technology requires major advancements due to the very large size of the various concepts (e.g., dimensions on the order of hundreds to thousands of kilometers).

Other critical technologies that will require significant (but not major) advancement include optical (e.g., high bandwidth) communications, power systems, and navigation. Payload power at megawatt levels could be met by advanced nuclear power systems. However, a very large (e.g., thousands of TW_e) power system may be required for the matter-antimatter propulsion system (e.g., electric power required during engine operation). More modest powers will be needed for energy storage systems for startup power, and housekeeping power during coast (for cryogenic refrigeration systems, electromagnetic storage of antimatter, etc.). Finally, navigation will require advancements in position knowledge (e.g., advanced optical navigation), timing (e.g., advanced highly-accurate and stable clocks), and acceleration (changes in position and time).

Finally, any long-duration space system will require a high level of reliability and system lifetime. With a requirement for systems to operate for decades to centuries, it may be necessary to re-think our

traditional assumptions about trading performance and lifetime. For example, instead of pursuing the goal of maximum performance, we may need to design systems for ease of maintenance, repair, or replacement, even if this means sacrificing some level of performance. Also, in the context of a highly intelligent robotic spacecraft, or ultimately a piloted mission, it is possible to imagine a completely autonomous vehicle where replacement parts are manufactured on the vehicle as needed; in effect, the vehicle would have its own "machine shop" and robots to perform the needed work. This also introduces the idea of sacrificing performance for ease of manufacturability in a completely autonomous robotic environment.

Public Outreach/Education Opportunities

Historically, there has been a fascination by the public for science-fiction and science-fact based on interstellar voyages and antimatter propulsion.[13] This suggests a powerful tool for engaging the general public in both the excitement and challenges of space exploration. Possibly the most important benefit is the education potential for class projects dealing with antimatter. There is, for example, the obvious charisma of antimatter (e.g., Star Trek et al.). Also, when done as a class project, a real-world engineering environment can be created with multi-disciplinary teams for each of the major subsystems: propulsion, power, thermal control (radiators, insulation, refrigeration), shielding, structures (tankage), etc. This can be used to demonstrate real-world problems like subsystem interfaces and interactions (e.g., interactions between the magnets, their shields, and radiators). Also, this gives the student experience in exploring all the various subtle issues that must be considered in assembling a complete vehicle; for example, until you do the calculation, you don't know if the Systems/Payload radiation shield is big enough to be self-radiating (from the heat produced by capture of gamma), or if you need to add dedicated radiators to dump the heat.

This type of class project also illustrates the kinds of tradeoffs encountered when seeking an optimum solution between conflicting (and often contradictory) requirements/demands. Also, because there is a strong emphasis on understanding the basic processes involved (e.g., sublimation, annihilation, relativistics), this type of project also demonstrates that Freshman Physics and Chemistry DO matter, even (especially?) for engineers. Further, from a practical point of view, there is enough data in the literature to make the class project feasible, while at the same time there is not too much data so that the student is encouraged (i.e., forced) to exercise his or her creativity and innovation in solving the problem. Finally, this type of project demonstrates the real-world problem that quite often you don't (can't?) know all the answers; you just have to take your best "educated" guess (but then check for the sensitivity or criticality of you assumptions).

Impact on Other Research

We have already mentioned several basic research topics suggested by this study, such as proton-antiproton annihilation product distribution, innovative annihilation reactions to produce more charged particles, techniques for improved production rate and efficiency, demonstration of "non-contact" methods to produce solid anti-H_2, and data on solid H_2 sublimation at low temperatures. Another result of these analyses suggests an alternative method in the Search for Extraterrestrial Intelligence (SETI). Specifically, most SETI searches have been done at radio frequencies. However, searches at optical frequencies might detect interstellar vehicle communications (or power-beaming for Laser Sails). In the case of the antimatter rocket, a search for 200 MeV gamma rays characteristic of the proton-antiproton annihilation might prove fruitful. This would have the advantage that although electron-positron gamma emission has been detected from natural sources (e.g., around the event horizon of Black Holes where the inward-spiraling matter in the accretion disk is heated to such high temperatures that spontaneous electron-positron pair production occurs), proton-antiproton annihilation should not occur naturally because of the unique conditions required for antiproton production. A confirmation of a technological origin of the gammas might also be obtained if a red- or blue-shift was observed matching acceleration or deceleration to/from 0.5c.

Societal Investments in Interstellar Missions

Given the inherent scale of any interstellar mission, one question that can be asked is what resources will a civilization be willing to expend on an interstellar mission? To try and answer this question, we used historical data for the U.S. Gross National Product (GNP) and Federal budgets during the Apollo era to see how much we spend on "luxury" items like space exploration (or War?). It is somewhat ironic, but if "War is Diplomacy by Other Means," then Apollo was "War by Other Means." This virtually wartime priority given to the Space Race as part of the Cold War helped justify the enormous expenditures on human and robotic space exploration during this era. However, as shown in Figure 15, even during the "Good Old Days" of Apollo, NASA's budget was less than 0.75% of the U.S. GNP (now ~0.13%). For comparison, in 2001, total U.S. Pet Industry expenditures were $28.5B; NASA's budget was less than one-half this ($13.4B).

As an alternative to NASA, we might consider military spending as a "luxury" that a saner civilization could divert to more productive uses. For example, starting in the 1960s, Defense spending has been

decreasing from 9% of the GNP (during the height of the Cold War) to today's 3% of GNP. In this context, Sir Arthur C. Clarke has described the state of humanity in his fictional worlds of 2001: "Mankind had finally found something [space exploration] as expensive, and as much *fun*, as war . . ." This suggests that a wiser human society might find more interesting uses for military spending.

More generally, it is worth noting that any civilization capable of marshalling the technologies and energies required for an Interstellar Mission had better be grown up! For comparison, the energy content of annihilating the antimatter in the 4-stage antimatter rocket is capable of vaporizing on the order of 100 m of the entire surface of the Earth. In fact, the ability of a civilization to destroy itself has been an on-going issue with estimating the lifetime of a technological civilization for use in the Drake Equation.

Based on these arguments, baring an impending disaster of Solar System wide proportions, we can estimate that around ~10% of a civilization's resources might be applied to an interstellar mission. Of course, something capable of rendering the Solar System uninhabitable (a nearby supernova?) might dramatically increase the priority of humanity's investment in an interstellar mission, just as the threat to survival that the Cold War represented increased the priority for Apollo.

SUMMARY

An interstellar mission is enormously difficult, but it is not impossible. It is, however, a civilization-defining challenge, with energies and powers thousands of times that of humanity today (e.g., current human civilization produces and consumes about 440 exajoules [440×10^{18} J] per year, corresponding to an average power level of 14 TW). The late Dr. Robert Forward put it most succinctly when he said that an interstellar mission would require "kilograms of energy." Normally, we don't think of energy in units of mass, yet this is a perfectly reasonable, if dramatic, way to look at the problem. In the case of the antimatter rocket, we will require millions of tons of energy (as antimatter), and the technological challenges of producing that much stored "energy" are formidable, but they are not in and of themselves impossible. What may be of more significance is the sheer size of any interstellar mission.

In the near term, development of the technologies required for an interstellar mission would represent a national (international?) goal that could focus NASA, DoE, DoD, Academia, and Industrial expertise. In the long term, it will represent a Solar System civilization's defining accomplishment in much the same way we look to the past accomplishments of humanity, like the Pyramids, Stonehenge, the great medieval Cathedrals of Europe, the Great Wall of China, and, not so long ago, a space program called Apollo.

In fact, it is encouraging that previous studies have identified not just one but three propulsion concepts that are capable of fast (~0.5c) interstellar rendezvous missions (Laser Sail, Antimatter, and Fusion Ramjet). This "Vision" mission is significantly more difficult than "slow" (0.1 c) interstellar flybys, which could be performed by a wide variety of propulsion technologies. However, all three of the leading candidates capable of performing the Vision mission have major unresolved feasibility issues. Given our current knowledge, there is no clear winner. Thus, near-term goals should seek to resolve fundamental feasibility issues with each of these concepts.

Recommended Further Work

Recommended additional systems modeling and analysis work needed for the Antimatter Rocket includes propellant storage and feed system (tankage, antimatter levitation and feed system), antimatter rocket engine electric power requirements, electric power system mass scaling, structure requirements (options, mass, and power for active structure control), dust shield spalling, Monte-Carlo gamma ray scattering calculations, and modeling of the miscellaneous spacecraft systems and payload. Recommended experimental research areas include improved measurements of proton-antiproton annihilation product distribution and demonstration of improved techniques for production and storage of antimatter.

Interstellar Mission Stretch Goal

Finally, it is worth noting that we wanted to generate a "Stretch Goal" based on an intentionally very difficult interstellar mission. Given the enormous technology and resource requirements that such a mission would require, we think that we succeeded. However, it is not unreasonable to ask whether we have designed Jules Verne's Cannon (way too big) or his Projectile (about right). We have only just begun to look at potential technology improvements that could dramatically reduce the current estimates of the size of the antimatter rocket; additional work will be needed to better understand this concept in order to identify a preferred propulsion approach for interstellar missions.

As an example of the need for improvements needed in the antimatter propulsion system, we can consider the characteristics of the 10X better radiator and magnet vehicle described above. The full 4-stage vehicle requires a total antiproton propellant load of 39,300,000 MT. The annihilation (MC^2) energy of this much antimatter (plus an equal amount of matter) corresponds to ~17.7 million years of current Human energy output. At current production efficiencies (10^{-9}), the energy required to produce the antiprotons

corresponds to ~17.7 quadrillion [10^{15}] years of current Human energy output. For comparison, this is "only" 590 years of the total energy output of sun. Even at the maximum predicted energy efficiency of antiproton production (0.01%), we would need 177 billion years of current Human energy output for production. In terms of production rate, we only need about $4x10^{21}$ times the current annual antiproton production rate. Finally, the 123,000 TW of first-stage engine "jet" power implies a need to dump 207,000 TW of 200 MeV γ-rays, again suggesting the need for dramatic improvements in radiator technology.

ACKNOWLEDGMENTS

This research was carried out at the Jet Propulsion Laboratory (JPL), California Institute of Technology, under a contract with the National Aeronautics and Space Administration (NASA).

I would like to thank Robert Miyake (JPL) for his thermal analyses of the propellant tanks, insulation systems, radiators, and sorption-compressor refrigerators, and Insoo Jun (JPL) who provided data for the radiation shielding requirements. Finally, I wish to thank John Cole (Head of the Revolutionary Propulsion Program at NASA Marshall Spaceflight Center) for providing overall funding support for this task in previous years. Although the Revolutionary Propulsion Program was cancelled in fiscal year 2003, we hope that it will be reinitiated in coming years so as to provide an opportunity to continue investigation of this and other advanced propulsion concepts for interstellar missions.

REFERENCES

[1] Frisbee, R.H., and Leifer, S.D., "Evaluation of Propulsion Options for Interstellar Missions," AIAA Paper AIAA-98-3403, Presented at the 34th AIAA/ASME/SAE/ASEE Joint Propulsion Conference & Exhibit, Cleveland OH, July 13-15, 1998.

[2] TRW Space Log, W.A. Donop Jr., Ed., Vol. 9, No. 4, Winter 1969-1970.

[3] As a literary side note, it is interesting that the "high-tech" weapons of the American Civil War, the cannon (and submarine), became the technology "gimmick" used by Verne in writing a fictional account of a trip to the Moon (and world-spanning submarine); similarly, 80 years later (1945), the high-tech weapons of World War II, rockets and atomic power, became the staple of science fiction writers of the post-war era (e.g., Robert Heinlein's Destination Moon).

[4] Forward, R.L., "Antiproton Annihilation Propulsion," AIAA Paper AIAA-84-1482, Presented at the AIAA/SAE/ASME 20th Joint Propulsion Conference, Cincinnati OH, June 11-13, 1984; and Air Force Rocket Propulsion Laboratory (AFRPL) Technical Report AFRPL TR-85-034, September 1985.

[5] Smith, G.A., et al., "Antiproton-Catalyzed Micro-fission/Fusion Propulsion Systems for Exploration of the Outer Solar System and Beyond," AIAA Paper AIAA 96-3069, Presented at the AIAA/ASME/SAE/ASEE 32nd Joint Propulsion Conference, Lake Buena Vista FL, July 1-3, 1996.

[6] Paine, C., and Seidel, G., "Brown University Magnetic Levitation / Supercooling Research," Presented at the NASA Office of Advanced Concepts and Technology (OACT) Third Annual Workshop on Advanced Propulsion Concepts, Pasadena CA, January 30-31, 1992, Proceedings published as JPL Internal Document JPL D-9416, R.H. Frisbee, Ed., 1992.

[7] Orth, C., et al., "Transport Vehicle for Manned Mars Missions Powered by Inertial Confinement Fusion," AIAA Paper 87-1904, Presented at the AIAA/SAE/ASME/ASEE 23rd Joint Propulsion Conference, San Diego CA, June 29-July 2, 1987.

[8] Callas, J.L., "The Application of Monte Carlo Modeling to Matter-Antimatter Annihilation Propulsion Concepts," JPL Internal Document D-6830, October 1, 1989.

[9] Morgan, D.L., "Concepts for the Design of an Antimatter Annihilation Rocket," J. British Interplanetary Soc., Vol. 35, pp. 414-421, 1982.

[10] Cooksey, J.W., et al., "Gamma-ray and Fast Neutron Radiation Effects on Thin Film Superconductors," IEEE Trans. on Nuclear Science, Vol. 41, No. 6, pp. 2521-2524, December 1994.

[11] Draine, B.T., and Lee, H.M., "Optical Properties of Interstellar Graphite and Silicate Grains," Astrophysical J., Vol. 285, pp. 89-108, October 1, 1984.

[12] LaPointe, M.R., "Antiproton Powered Propulsion with Magnetically Confined Plasma Engines," J. Propulsion, Vol. 7, No. 5, pp. 749-759, September-October 1991.

[13] Weed, W.S., "Can We Rocket to Another Star?," Discover, Vol. 24, No. 8, pp. 34-41, August 2003.

Table 12. Summary of 40 LY Mission Data

Stage Number **Stage Parameters**	**Stage 4** Nominal	**Stage 4** 10X Better Rad&Mag	**Stage 3** Nominal	**Stage 3** 10X Better Rad&Mag	**Stage 2** Nominal	**Stage 2** 10X Better Rad&Mag	**Stage 1** Nominal	**Stage 1** 10X Better Rad&Mag
Payload Values for This Stage								
Payload Mass for Stage "N" (MT)	100	100	386,684	89,895	5,296,499	1,086,312	52,100,499	9,824,463
Payload Power Pe (MWe)	10	10	0	0	0	0	0	0
Basic Mission Parameters (Same for All Values of Standoff Distance X)								
ΔV for this Stage (%c)	25.00%	25.00%	25.00%	25.00%	25.00%	25.00%	25.00%	25.00%
Isp (%c)	33.33%	33.33%	33.33%	33.33%	33.33%	33.33%	33.33%	33.33%
Mo/Mb (Relativistic, a=0.2230)	5.45081	5.45081	5.45081	5.45081	5.45081	5.45081	5.45081	5.45081
Average Acceleration (gees)	0.010	0.010	0.010	0.010	0.010	0.010	0.010	0.010
(m/s^2)	0.098	0.098	0.098	0.098	0.098	0.098	0.098	0.098
No. of Stages per Accel or Decel Step	2	2	2	2	2	2	2	2
Mission Duration (Years)	128.50	128.50	104.25	104.25	48.50	48.50	24.25	24.25
Acceleration	48.50	48.50	48.50	48.50	48.50	48.50	24.25	24.25
Coast	31.50	31.50	31.50	31.50	0.00	0.00	0.00	0.00
Deceleration	48.50	48.50	24.25	24.25	0.00	0.00	0.00	0.00
Engine Run Time	24.25	24.25	24.25	24.25	24.25	24.25	24.25	24.25
Distances (LY)	40.00	40.00	36.97	36.97	12.13	12.13	3.03	3.03
Acceleration	12.13	12.13	12.13	12.13	12.13	12.13	3.03	3.03
Coast	15.75	15.75	15.75	15.75				
Deceleration	12.13	12.13	9.09	9.09				
Totals for Dust Impact Shield Calculations								
Time (Years)	128.50	128.50	104.25	104.25	48.50	48.50	24.25	24.25
Distance (LY)	40.00	40.00	36.97	36.97	12.13	12.13	3.03	3.03
Max Velocity (%c)	0.50	0.50	0.50	0.50	0.50	0.50	0.25	0.25
Dry Mass Calculations (These Quantities Depend on X)								
Magnet, Shield, Radiator								
Initial X =	1.000	1.000	2.000	2.000	5.000	5.000	10.000	10.000
Delta X =	0.025	0.025	0.075	0.075	0.200	0.200	1.000	1.000
Optimum (Minimum Mass) Distance Values								
Standoff Distance(X) (m)	4.975	2.600	13.400	6.425	35.000	15.400	83.000	34.000
Coil Radius (R) (m)	9.950	5.200	26.800	12.850	70.000	30.800	166.000	68.000
Mag Center Dist (m) to Ignition Point	11.124	5.814	29.963	14.367	78.262	34.435	185.594	76.026
Engine Parameters Based on Average Acceleration and Dry Mass								
Thrust, F (N)	1.175E+07	2.731E+06	1.609E+08	3.301E+07	1.583E+09	2.985E+08	1.382E+10	2.453E+09
Jet Power, Pjet (TW)	587.4	136.6	8,046.4	1,650.3	79,150.5	14,925.2	691,134.0	122,648.0
Total Charged Pion Flow Rate (kg/s) = F/Isp	0.1175	0.0273	1.6093	0.3301	15.8301	2.9850	138.2268	24.5296
Total Charged Pion MC^2 Flow Rate (TW π+/-)	10,574.0	2,458.2	144,835.0	29,705.6	1,424,710	268,654	12,440,412	2,207,663
Engine Power Values								
Total Charged Pion MC^2 Flow Rate (TW π+/-)	587.4	136.6	8,046.4	1,650.3	79,150.5	14,925.2	691,134.0	122,648.0
Total Gamma Power (TW of 200 MeV Gammas)	996.3	231.6	13,646.4	2,798.9	134,236	25,313	1,172,138	208,007
Total MC^2 Power (T-W = T-J/s)	2,634.3	612.4	36,082.5	7,400.5	354,935	66,929	3,099,256	549,991
Total H/H_ Mass Flow Rate (M-DOT) (kg/s)	2.927E-02	6.805E-03	4.009E-01	8.223E-02	3.944E+00	7.437E-01	3.444E+01	6.111E+00
Total H/H_ Atom Flow Rate (H+/H- Pairs per sec)	8.810E+24	2.048E+24	1.207E+26	2.475E+25	1.187E+27	2.238E+26	1.037E+28	1.839E+27
Number of Gammas per H+/H-	4	4	4	4	4	4	4	4
Total Gammas/sec	3.52E+25	8.19E+24	4.83E+26	9.90E+25	4.75E+27	8.95E+26	4.15E+28	7.36E+27
Run Time (Years)	24.25	24.25	24.25	24.25	24.25	24.25	24.25	24.25
Total Number of 200 MeV Gammas Produced	2.70E+34	6.27E+33	3.69E+35	7.58E+34	3.63E+36	6.85E+35	3.17E+37	5.63E+36
Calculation of H+ or H_ Ion Beam Tube Diameter								
Space-Charge Ion Limit (Ions/cc)	1.000E+10	1.000E+10	1.000E+10	1.000E+10	1.000E+10	1.000E+10	1.000E+10	1.000E+10

Total H+ OR H- Ion Number Flow Rate (Ions/sec)	8.810E+24	2.048E+24	1.207E+26	2.475E+25	1.187E+27	2.238E+26	1.037E+28	1.839E+27
Total H+ OR H- Ion Volume Flow Rate (cc/sec)	8.810E+14	2.048E+14	1.207E+16	2.475E+15	1.187E+17	2.238E+16	1.037E+18	1.839E+17
Assumed Ion Velocity (%c)	0.10%	0.10%	0.10%	0.10%	0.10%	0.10%	0.10%	0.10%
Ion Stream Cross-Section Dia. (m)	61.15	29.48	226.31	102.49	709.79	308.22	2,097.42	883.56
Total Power Required to Vaporize SH2 or LH2, Dissociate H2 into Atoms, Ionize the Atoms, and Accelerate the Ions Down the Beam								
Total Energy (J/kg)	4.653E+10	4.653E+10	4.653E+10	4.653E+10	4.653E+10	4.653E+10	4.653E+10	4.653E+10
Total Power Pe (kW = J/s/1000)	1.513E+06	3.518E+05	2.073E+07	4.251E+06	2.039E+08	3.845E+07	1.780E+09	3.159E+08
Engine Miscl Power (Based on 10^-6 Fraction of Total MC^2 Power)								
Engine Miscl Power (kWe)	2.634E+06	6.124E+05	3.608E+07	7.401E+06	3.549E+08	6.693E+07	3.099E+09	5.500E+08

Magnet, Magnet Structure, and Magnet Thermal Control (Insulation, Refrigerator)

Magnet Dimensions								
Required Current (I) (Amps)	1.958E+09	1.023E+09	5.273E+09	2.528E+09	1.377E+10	6.060E+09	3.266E+10	1.338E+10
Cross-Sectional Area (m^2)	0.196	0.010	0.527	0.025	1.377	0.061	3.266	0.134
Length (a) (m)	0.626	0.143	1.027	0.225	1.660	0.348	2.556	0.517
Width (b) (m)	0.313	0.072	0.513	0.112	0.830	0.174	1.278	0.259
Min. Distance (m) to Ignition Point	10.812	5.742	29.450	14.254	77.433	34.261	184.316	75.768
Volume (m^3)	12.239	0.334	88.792	2.041	605.762	11.728	3,406.611	57.164
Mass (MT)	61.196	1.671	443.962	10.207	3,028.81	58.64	17,033.05	285.82
Magnet Structure (Carbon Nanotube)								
Effective Structure Radius = R-Coil + (Magnet Length a)/2 (m)	10.263	5.272	27.313	12.962	70.830	30.974	167.278	68.259
Structure Thickness (m)	3.120	1.602	8.303	3.940	21.530	9.415	50.848	20.749
Structure Volume (m^3)	112.587	6.791	1,308.761	64.545	14,223.97	570.57	122,171.68	4,117.27
Structure Mass (MT)	213.915	12.902	2,486.647	122.636	27,025.55	1,084.09	232,126.20	7,822.81
Magnet Insulation (1500->100 K)								
Surface Area of Magnet (m^2)	681.50	176.95	4,774.29	1,064.83	31,887.97	6,061.78	177,150.91	29,385.50
Insulation Mass (MT)	7.156	1.858	50.130	11.181	334.824	63.649	1,860.085	308.548
Cooling Load (Wcool) from Hot Shield	370,735	96,260	2,597,216	579,266	17,347,057	3,297,607	96,370,097	15,985,710
Magnet Refrigerator (100 K)								
Pe (We)	3.707E+06	9.626E+05	2.597E+07	5.793E+06	1.735E+08	3.298E+07	9.637E+08	1.599E+08
Mass (MT)	3,707	963	25,972	5,793	173,471	32,976	963,701	159,857
Effective Radiator Area (m^2)	2.605	0.676	18.247	4.070	121.877	23.168	677.075	112.312
2-Side 1-Plate Fin&Tube Radiator Length (m)	0.131	0.065	0.340	0.158	0.871	0.376	2.039	0.826

Radiation (Gamma) Shields

Geometric Fraction of Total Gamma Number Flux Intercepted by Magnet								
Fraction = Aring/Asphere	1.294%	0.557%	0.780%	0.353%	0.479%	0.227%	0.310%	0.153%
Number Gammas Intercepted	3.490E+32	3.493E+31	2.880E+33	2.673E+32	1.742E+34	1.557E+33	9.839E+34	8.596E+33
Magnet Shield (1500K) Dimensions								
Thickness [Length] (t) (m)	0.173	0.172	0.176	0.175	0.178	0.178	0.180	0.180
Shield Attenuation Factor	8.496E-15	1.031E-14	4.602E-15	5.257E-15	3.235E-15	3.358E-15	2.099E-15	1.999E-15
Magnet Side Shield Thickness (t') (m)	0.017	0.017	0.018	0.018	0.018	0.018	0.018	0.018
Min. Distance (m) to Ignition Point	10.639	5.571	29.274	14.079	77.255	34.084	184.136	75.587
Shield Center Dist (m) to Ign. Point	11.038	5.728	29.875	14.279	78.173	34.347	185.504	75.936
Cross-Sectional Area (m^2) - Amag	0.088	0.025	0.142	0.036	0.228	0.053	0.352	0.077
Volume (m^3)	5.337	0.796	23.626	2.900	99.576	10.258	365.617	32.841
Mass (MT)	103.268	15.406	457.163	56.116	1,926.794	198.484	7,074.687	635.468
Geometric Fraction of Total Gamma Power Flux Intercepted by Magnet Shield								
Fraction = Aring/Asphere	1.460%	0.850%	0.838%	0.468%	0.501%	0.275%	0.319%	0.174%
Gammas Power Intercepted (GW)	1.455E+04	1.968E+03	1.144E+05	1.311E+04	6.725E+05	6.961E+04	3.740E+06	3.627E+05
Main Radiator Shield (1500K) Dimensions								
Min. Distance (m) to Ignition Point (Along Hypot.)	11.455	5.902	30.494	14.497	79.110	34.627	186.890	76.303
Min. Distance (m) to Ignition Point (Along Standoff=X Axis)	5.123	2.640	13.637	6.483	35.379	15.486	83.580	34.124
Height=2R (m)	19.900	10.400	53.600	25.700	140.000	61.600	332.000	136.000
Width (m)	0.125	0.125	0.125	0.125	0.125	0.125	0.125	0.125
Cross-Sectional Area (m^2)	2.488	1.300	6.700	3.213	17.500	7.700	41.500	17.000
Shield Attenuation Factor	1.272E-11	1.452E-11	6.580E-12	7.250E-12	4.502E-12	4.574E-12	2.877E-12	2.703E-12
Thickness (t2) (m)	0.134	0.133	0.137	0.137	0.139	0.139	0.142	0.142
Volume (m^3)	0.332	0.173	0.919	0.439	2.436	1.071	5.876	2.413
Mass (MT)	6.434	3.345	17.784	8.495	47.136	20.727	113.694	46.683

Geometric Fraction of Total Gamma Power Flux Intercepted by Radiator Shield								
Fraction = Arectangle/Asphere	0.151%	0.297%	0.057%	0.122%	0.022%	0.051%	0.009%	0.023%
Gammas Power Intercepted (GW)	1.503E+03	6.877E+02	7.824E+03	3.405E+03	2.987E+04	1.294E+04	1.108E+05	4.833E+04
Payload Shield Dimensions								
Min. Distance (m) to Ign. Point	5.152E+05	1.631E+05	1.456E+06	4.105E+05	3.204E+06	8.559E+05	7.409E+06	1.930E+06
Radius=R (m)	9.950	5.200	26.800	12.850	70.000	30.800	166.000	68.000
Cross-Sectional Area (m^2)	311.026	84.949	2,256.418	518.748	15,393.80	2,980.24	86,569.73	14,526.72
Thickness (t3) (m)	0.060	0.064	0.063	0.068	0.067	0.072	0.069	0.074
Shield Attenuation Factor	1.286E-05	5.545E-06	7.502E-06	2.906E-06	3.693E-06	1.397E-06	2.261E-06	8.649E-07
Volume (m^3)	18.661	5.478	141.861	35.235	1,025.94	214.05	5,995.77	1,080.49
Mass (MT)	361.09	105.99	2,745.00	681.79	19,851.94	4,141.95	116,018.20	20,907.56
Shield as 1-Sided Rad. Area. (m^2)	311.026	84.949	2,256.418	518.748	15,393.80	2,980.24	86,569.73	14,526.72
Waste Heat Emitted (GW)	4.133E-07	4.133E-07	4.133E-07	4.133E-07	4.133E-07	4.133E-07	4.133E-07	4.133E-07
Geometric Fraction of Total Gamma Power Flux Intercepted by Payload Shield								
Fraction = Adisk/Asphere	9.325E-11	2.541E-10	8.468E-11	2.450E-10	1.193E-10	3.238E-10	1.255E-10	3.102E-10
Number Gammas Intercepted	2.515E+24	1.593E+24	3.128E+25	1.857E+25	4.336E+26	2.218E+26	3.982E+27	1.747E+27
Gammas Power Intercepted (GW)	9.290E-05	5.886E-05	1.156E-03	6.858E-04	1.602E-02	8.195E-03	1.471E-01	6.453E-02
Payload Shield Radiator Dimensions								
Total Gamma Pwr. Radiated (GW)	9.249E-05	5.844E-05	1.155E-03	6.854E-04	1.602E-02	8.195E-03	1.471E-01	6.453E-02
2-Sided Radiator Eff. Area (m^2)	111.880	70.694	1,397.292	829.088	19,372.993	9,912.746	177,925.574	78,058.096
Radiator Length (Width=2R) (m)	5.622	6.798	26.069	32.260	138.379	160.921	535.920	573.957
Radiator Mass (MT)	0.559	0.353	6.986	4.145	96.865	49.564	889.628	390.290

Main Radiator Dimensions (1500K, to Radiate Gamma Power Absorbed by Magnet and Main Radiator Shields)

Total Gamma Pwr. Intercepted (GW)	16,052	2,656	122,203	16,515	702,345	82,543	3,851,312	411,023
2-Sided Radiator Eff. Area (m^2)	1.025E+07	1.696E+06	7.805E+07	1.055E+07	4.486E+08	5.272E+07	2.460E+09	2.625E+08
Radiator Length (Width=2R) (km)	515.189	163.100	1,456.190	410.446	3,204.234	855.861	7,409.221	1,930.319
Radiator Mass (MT)	15,533.7	257.0	118,260.3	1,598.3	679,686	7,988	3,727,063	39,776

Propellant Tankage, Insulation, Refrigerators

Total Useable Mp (LH2+Anti-SH2) (MT)								
	315,743	73,403	4,324,808	887,018	42,542,190	8,022,076	371,473,816	65,921,382
LH2 Propellant Load (1/2 Total Useable Mp)								
Total Useable Propellant Mass (MT)	157,872	36,701	2,162,404	443,509	21,271,095	4,011,038	185,736,908	32,960,691
Losses, Boiloff (MT)	1,579	367	21,624	4,435	212,711	40,110	1,857,369	329,607
Total Propellant Mass (MT)	159,450	37,068	2,184,028	447,944	21,483,806	4,051,148	187,594,277	33,290,298
Total Propellant Volume (m^3)	2.278E+06	5.295E+05	3.120E+07	6.399E+06	3.069E+08	5.787E+07	2.680E+09	4.756E+08
Anti-SH2 Propellant Load (1/2 Total Useable Mp)								
Total Useable Propellant Mass (MT)	157,872	36,701	2,162,404	443,509	21,271,095	4,011,038	185,736,908	32,960,691
Losses, Boiloff (MT)	7,894	1,835	108,120	22,175	1,063,555	200,552	9,286,845	1,648,035
Total Propellant Mass (MT)	165,765	38,536	2,270,524	465,684	22,334,650	4,211,590	195,023,754	34,608,726
Total Propellant Volume (m^3)	2.368E+07	5.505E+06	3.243E+08	6.652E+07	3.190E+09	6.016E+08	2.786E+10	4.944E+09
LH2 Tank Dimensions								
Volume w/ Ullage (m^3)	2.392E+06	5.560E+05	3.276E+07	6.719E+06	3.223E+08	6.077E+07	2.814E+09	4.994E+08
Cylinder L (m)	7,677	6,538	14,483	12,936	20,841	20,349	32,283	34,284
End-Domes L (m)	19.9	10.4	53.6	25.7	140.0	61.6	332.0	136.0
Total Length (m)	7,697	6,549	14,537	12,961	20,981	20,411	32,615	34,420
Cylinder A (m^2)	479,925	213,629	2,438,791	1,044,400	9,166,295	3,937,976	33,671,728	14,648,158
End-Domes A (m^2)	1,244	340	9,026	2,075	61,575	11,921	346,279	58,107
Total Area (m^2)	481,169	213,969	2,447,816	1,046,475	9,227,871	3,949,897	34,018,007	14,706,265
Anti-SH2 Tank Dimensions								
Volume w/ Ullage (m^3)	2.368E+07	5.505E+06	3.243E+08	6.652E+07	3.190E+09	6.016E+08	2.786E+10	4.944E+09
Cylinder L (m)	76,116	64,792	143,698	128,212	207,152	201,818	321,570	340,216
End-Domes L (m)	19.9	10.4	53.6	25.7	140.0	61.6	332.0	136.0
Total Length (m)	76,136	64,802	143,752	128,238	207,292	201,879	321,902	340,352
Cylinder A (m^2)	4,758,575	2,116,915	24,197,249	10,351,735	91,110,427	39,056,166	335,400,114	145,359,552
End-Domes A (m^2)	1,244	340	9,026	2,075	61,575	11,921	346,279	58,107
Total Area (m^2)	4,759,819	2,117,255	24,206,275	10,353,810	91,172,002	39,068,087	335,746,393	145,417,659
LH2 Tank and Insulation Masses								
Insulation & Thermal Shield Mass (MT)	481	214	2,449	1,047	9,238	3,952	34,072	14,715
Tank Mass (MT)	650	289	3,305	1,413	12,458	5,332	45,924	19,853
Losses, Boiloff (MT)	1,579	367	21,624	4,435	212,711	40,110	1,857,369	329,607
Total (MT)	2,710	870	27,378	6,895	234,406	49,395	1,937,366	364,176
Tankage Factor (%)	1.72%	2.37%	1.27%	1.55%	1.10%	1.23%	1.04%	1.10%
Miscl Structure, Feed, Pressurant, etc. (MT)								
	1,595	371	21,840	4,479	214,838	40,511	1,875,943	332,903
Tankage Factor (%)	1.01%	1.01%	1.01%	1.01%	1.01%	1.01%	1.01%	1.01%

Total Tank, Insulation, Structure, Feed, Press, etc. (MT)								
	4,304	1,241	49,218	11,374	449,244	89,906	3,813,309	697,079
Tankage Factor (%)	2.73%	3.38%	2.28%	2.56%	2.11%	2.24%	2.05%	2.11%
Anti-SH2 Tank and Insulation Masses								
Insulation & Thermal Shield Mass (MT)	4,760	2,117	24,208	10,354	91,182	39,070	335,801	145,427
Tank Mass (MT)	6,426	2,858	32,678	13,978	123,082	52,742	453,258	196,314
Losses, Boiloff (MT)	7,894	1,835	108,120	22,175	1,063,555	200,552	9,286,845	1,648,035
Total (MT)	19,079	6,811	165,006	46,507	1,277,819	292,364	10,075,904	1,989,775
Tankage Factor (%)	12.09%	18.56%	7.63%	10.49%	6.01%	7.29%	5.42%	6.04%
Miscl Structure, Feed, Pressurant, etc. (MT)								
	3,315	771	45,410	9,314	446,693	84,232	3,900,475	692,175
Tankage Factor (%)	2.10%	2.10%	2.10%	2.10%	2.10%	2.10%	2.10%	2.10%
Total Tank, Insulation, Structure, Feed, Press, etc. (MT)								
	22,395	7,581	210,417	55,821	1,724,512	376,596	13,976,379	2,681,950
Tankage Factor (%)	14.19%	20.66%	9.73%	12.59%	8.11%	9.39%	7.52%	8.14%
LH2 Tank Refrigerators								
Cooling Load (Wcool)	-	-	-	-	-	-	-	-
Refrigerator								
Pe (We)	-	-	-	-	-	-	-	-
Mass (MT)	-	-	-	-	-	-	-	-
Effective Radiator Area (m^2)	-	-	-	-	-	-	-	-
2-Side 1-Plate Fin&Tube Radiator Length (m)								
	-	-	-	-	-	-	-	-
Anti-SH2 Tank Refrigerators								
Cooling Load (Wcool)	104.72	46.58	532.54	227.78	2,005.78	859.50	7,386.42	3,199.19
Refrigerator								
Pe (We)	1.047E+06	4.658E+05	5.325E+06	2.278E+06	2.006E+07	8.595E+06	7.386E+07	3.199E+07
Mass (MT)	104.72	46.58	532.54	227.78	2,005.78	859.50	7,386.42	3,199.19
Effective Radiator Area (m^2)	1,266.82	563.51	6,442.49	2,755.66	24,265.4	10,397.9	89,358.7	38,702.8
2-Side 1-Plate Fin&Tube Radiator Length (m)								
	63.66	54.18	120.20	107.22	173.32	168.80	269.15	284.58
Note: The Following are for Comparison of Total Tankage Factors with Contingency - Final Contingency Taken at End of Calculations								
LH2 Tank,Insulation,Struct,Refrig Masses w/ Contingency								
Tank, Insulation, Refrig, Structure, etc. (MT)								
	4,304.16	1,240.58	49,218.1	11,374.1	449,244	89,906	3,813,309	697,079
30% Contingency (MT)	1,291.25	372.17	14,765.4	3,412.2	134,773	26,972	1,143,993	209,124
Grand Total w/ Contingency (MT)	5,595.41	1,612.75	63,983.5	14,786.3	584,017	116,878	4,957,301	906,202
Tankage Factor (%)	3.54%	4.39%	2.96%	3.33%	2.75%	2.91%	2.67%	2.75%
Anti-SH2 Tank,Insulation,Struct,Refrig Masses w/ Contingency								
Tank, Insulation, Refrig, Structure, etc. (MT)								
	22,499.36	7,627.97	210,949.4	56,048.7	1,726,517	377,455	13,983,765	2,685,149
30% Contingency (MT)	6,749.81	2,288.39	63,284.8	16,814.6	517,955	113,237	4,195,130	805,545
Grand Total w/ Contingency (MT)	29,144.46	9,869.79	273,701.7	72,635.5	2,242,467	489,832	18,171,509	3,487,494
Tankage Factor (%)	9.23%	13.45%	6.33%	8.19%	5.27%	6.11%	4.89%	5.29%
Grand Total LH2+Anti-SH2 Tanks, Insulation, Refrig, Structure, Contingency, etc.								
Grand Total Mass (MT)	34,739.86	11,482.54	337,685.23	87,421.82	2,826,484	606,710	23,128,810	4,393,697
Grand Total Tankage Factor (%)	11.00%	15.64%	7.81%	9.86%	6.64%	7.56%	6.23%	6.67%
Miscl Spacecraft Systems (Avionics, Attitude Control, Telecommunications, etc.)								
Miscl Spacecraft Systems (MT)	100.00	100.00	100.00	100.00	100.00	100.00	100.00	100.00
Payload (Robotic)								
Payload (MT)	100.00	100.00	386,683.63	89,894.57	5,296,499	1,086,312	52,100,499	9,824,463
Additional Shielding for Human Payload (For Comparison Only; Not Used for Robotic Mission)								
Min. Distance (m) to Ignition Point	599,095	234,515						
Radius=R (m)	9.95	5.20						
Cross-Sectional Area (m^2)	311.026	84.949						
Thickness (t4) (m)	0.046	0.044						
Shield Attenuation Factor	1.640E-04	2.507E-04						
Total Attenuation Factor (w/ Payload Shield)								
	2.109E-09	1.390E-09						
Volume (m^3)	14.443	3.753						
Mass (MT)	279.469	72.612						

Cruise Power System

Summary of Power Requirements								
Engine Systems (Feed+Miscl) Pe (MWe)	4,147.56	964.21	56,810.12	11,651.75	558,829	105,377	4,879,631	865,935
Total Refrigerator Pe (MWe)	4.75	1.43	31.30	8.07	193.53	41.57	1,037.57	191.85
Miscl Systems Pe (MWe)	10.00	10.00	10.00	10.00	10.00	10.00	10.00	10.00
Payload Pe (MWe)	10.00	10.00	0.00	0.00	0.00	0.00	0.00	0.00
Total Pe (MWe)	4,172.31	985.64	56,851.41	11,669.82	559,032	105,429	4,880,679	866,136
Total Pe (MWe) Limit for Specific Mass Calcs	3,834	3,834	3,834	3,834	3,834	3,834	3,834	3,834
Power System Specific Mass (kg/kWe=MT/MWe)	0.255	0.503	0.255	0.255	0.255	0.255	0.255	0.255
Power System Mass (MT)	1,064.61	496.04	14,506.23	2,977.68	142,643	26,901	1,245,356	221,004
1-Side 1-Plate LDR Radiator Length (m)	11,239.1	5,080.3	56,857.0	24,341.0	214,050	91,745	788,042	341,393
Dust Impact Shield								
Shield Radius (R) (m) (w/ 50 % Radius Margin)	14.93	7.80	40.20	19.28	105.00	46.20	249.00	102.00
Radius of Upper Stage (m)	(None)	(None)	9.95	5.20	26.80	12.85	70.00	30.80
Maximum (Worst-Case) Speed (%c)	50.00%	50.00%	50.00%	50.00%	50.00%	50.00%	25.00%	25.00%
Mission Duration (Years)	128.50	128.50	104.25	104.25	48.50	48.50	24.25	24.25
Relativistic Correction	1.15	1.15	1.15	1.15	1.15	1.15	1.03	1.03
Energy/Mass (J/g)	1.30E+13	1.30E+13	1.30E+13	1.30E+13	1.30E+13	1.30E+13	2.90E+12	2.90E+12
Volume (cc) per cm^2 Shield Area per second at Max Speed	1.50E+10	1.50E+10	1.50E+10	1.50E+10	1.50E+10	1.50E+10	7.50E+09	7.50E+09
Tot. Vol. (cc) per Mission per cm^2 Area for Tot. Dist. Traveled	3.79E+19	3.79E+19	3.50E+19	3.50E+19	1.15E+19	1.15E+19	2.87E+18	2.87E+18
Mdust = g/cc per cm^2 of Shield Area	7.57E-27	7.57E-27	7.57E-27	7.57E-27	7.57E-27	7.57E-27	7.57E-27	7.57E-27
Mtotal dust = g/Mission per cm^2 Shield Area	2.87E-07	2.87E-07	2.65E-07	2.65E-07	8.69E-08	8.69E-08	2.17E-08	2.17E-08
Impact Energy (Joules) per cm^2 Area	3.72E+06	3.72E+06	3.44E+06	3.44E+06	1.13E+06	1.13E+06	6.31E+04	6.31E+04
For a Graphite (C) Dust Impact Shield (All values per cm^2 Shield Area)								
Energy (J) to Vaporize Graphite (C)	3.72E+06	3.72E+06	3.44E+06	3.44E+06	1.13E+06	1.13E+06	6.31E+04	6.31E+04
Mass (g) of Graphite (C) Evaporated	62.21	62.21	57.49	57.49	18.86	18.86	1.05	1.05
Mass (kg)	0.06	0.06	0.06	0.06	0.02	0.02	0.00	0.00
Total Impact Power (milli-Watts)	0.92	0.92	1.05	1.05	0.74	0.74	0.08	0.08
Depth of Graphite (C) Evaporated (cm)	27.65	27.65	25.55	25.55	8.38	8.38	0.47	0.47
cm Thickness (w/ 10 X Spalling Factor & 50 % Margin)	414.71	414.71	383.29	383.29	125.72	125.72	7.03	7.03
For Total Graphite (C) Dust Impact Shield (All values for Total Shield Area)								
Total Graphite (C) Shield Mass (g)	6.53E+09	1.78E+09	2.48E+10	5.37E+09	5.43E+10	9.88E+09	1.59E+10	2.52E+09
Mass (MT)	6,529.96	1,783.49	24,791.68	5,367.25	54,342.15	9,883.60	15,916.75	2,518.30
Total Impact Power (Watts)	6,426.67	1,755.28	53,114.40	12,210.94	255,461.93	49,457.43	160,620.62	26,952.74
Self Radiating (Yes/No)	Yes	Yes	Yes	Yes	Yes	Yes	Yes	Yes

Mass Summary (MT)

Dust Shield	6,530.0	1,783.5	24,791.7	5,367.3	54,342	9,884	15,917	2,518
Power System	1,064.6	496.0	14,506.2	2,977.7	142,643	26,901	1,245,356	221,004
Payload	100.0	100.0	386,683.6	89,894.6	5,296,499	1,086,312	52,100,499	9,824,463
Miscl Vehicle Systems	100.0	100.0	100.0	100.0	100	100	100	100
Propellant Tanks, Insulation, Feed System	26,698.8	8,822.0	259,635.0	67,195.0	2,173,756	466,502	17,789,688	3,379,028
Propellant Tank Refrigeration	104.7	46.6	532.5	227.8	2,006	859	7,386	3,199
Payload Shield (w/ Radiator)	361.6	106.3	2,752.0	685.9	19,949	4,192	116,908	21,298
Hot Shield Radiator	15,533.7	257.0	118,260.3	1,598.3	679,686	7,988	3,727,063	39,776
Radiator Shield	6.4	3.3	17.8	8.5	47	21	114	47
Magnet Shield	103.3	15.4	457.2	56.1	1,927	198	7,075	635
Magnet, Magnet Structure, and Magnet Insulation	282.3	16.4	2,980.7	144.0	30,389	1,206	251,019	8,417
Magnet Refrigerator	3,707.4	962.6	25,972.2	5,792.7	173,471	32,976	963,701	159,857
Subtotal (MT)	54,592.8	12,709.2	836,689.1	174,047.8	8,574,814	1,637,139	76,224,825	13,660,343

30% Contingency on Dry Mass w/o Payload (MT)	16,347.8	3,782.8	135,001.7	25,246.0	983,495	165,248	7,237,298	1,150,764
Grand Total Dry Mass (MT)	70,940.6	16,492.0	971,690.8	199,293.7	9,558,309	1,802,387	83,462,123	14,811,107
Check If Total Dry Mass Is Blowing-Up								
Dry Mass Limit (MT)	1,000,000.0	1,000,000.0	10,000,000.0	10,000,000.0	100,000,000	100,000,000	500,000,000	500,000,000
Total Calculated Dry Mass (MT)	70,940.6	16,492.0	971,690.8	199,293.7	9,558,309	1,802,387	83,462,123	14,811,107
Total Propellant Mass (MT)	315,743.0	73,402.6	4,324,808.4	887,017.9	42,542,190	8,022,076	371,473,816	65,921,382
Grand Total Wet Mass (MT)	386,683.6	89,894.6	5,296,499.2	1,086,311.6	52,100,499	9,824,463	454,935,939	80,732,490
Effective Tankage Fraction (w/o Payload)	22.44%	22.33%	13.53%	12.33%	10.02%	8.93%	8.44%	7.56%
Overall Vehicle Dimensions								
Standoff Distance(X) (m)	4.98	2.60	13.40	6.43	35.00	15.40	83.00	34.00
Coil Radius (R) (m)	9.95	5.20	26.80	12.85	70.00	30.80	166.00	68.00
Min. Distance to Ignition Point								
Payload Shield (km)	515.19	163.10	1,456.20	410.45	3,204.27	855.88	7,409.30	1,930.35
Radiator Shield (m)	11.45	5.90	30.49	14.50	79.11	34.63	186.89	76.30
Magnet Center (m)	11.12	5.81	29.96	14.37	78.26	34.44	185.59	76.03
Magnet Shield (m)	10.64	5.57	29.27	14.08	77.25	34.08	184.14	75.59

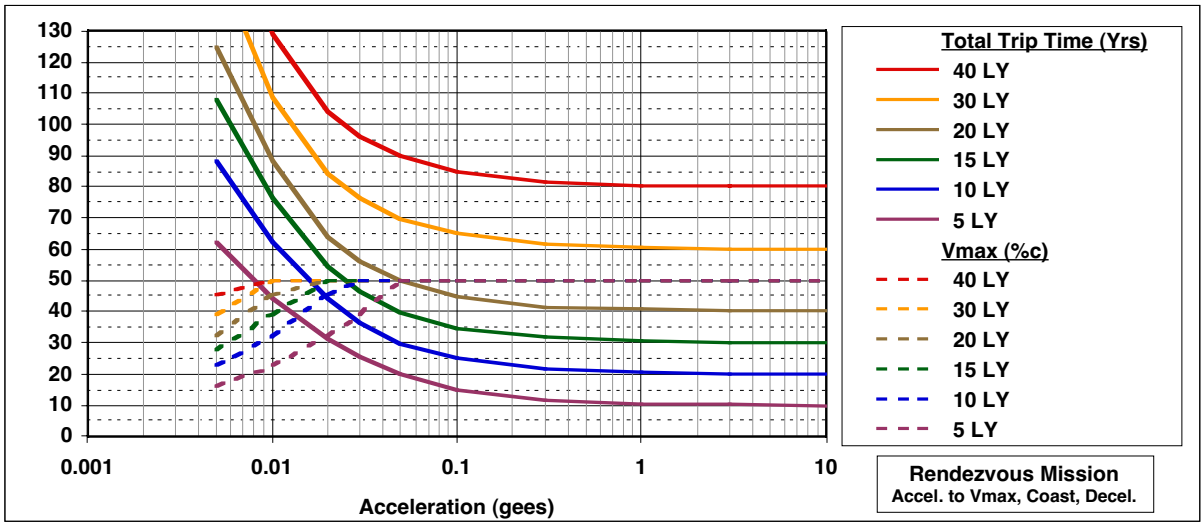

Figure 1. Impact of Acceleration and Mission Distance on Cruise Velocity and Trip Time for Interstellar Missions. (Rendezvous mission with acceleration, cruise, and deceleration.)

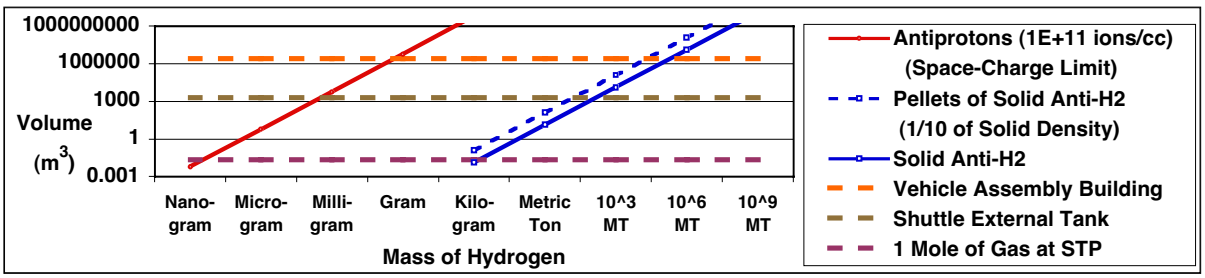

Figure 2. Storage Volume versus Hydrogen Mass for Space-Charge Limited H Ions and Solid H_2 Density.

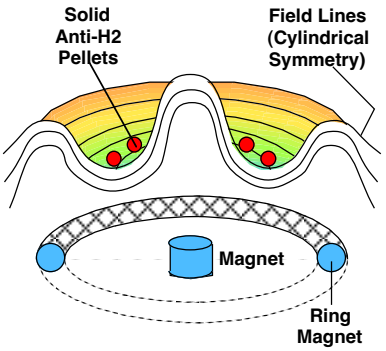

Figure 3. "Sombrero" Magnetic Field Geometry Used for Magnetic Levitation of Normal-Matter LH_2 and SH_2.

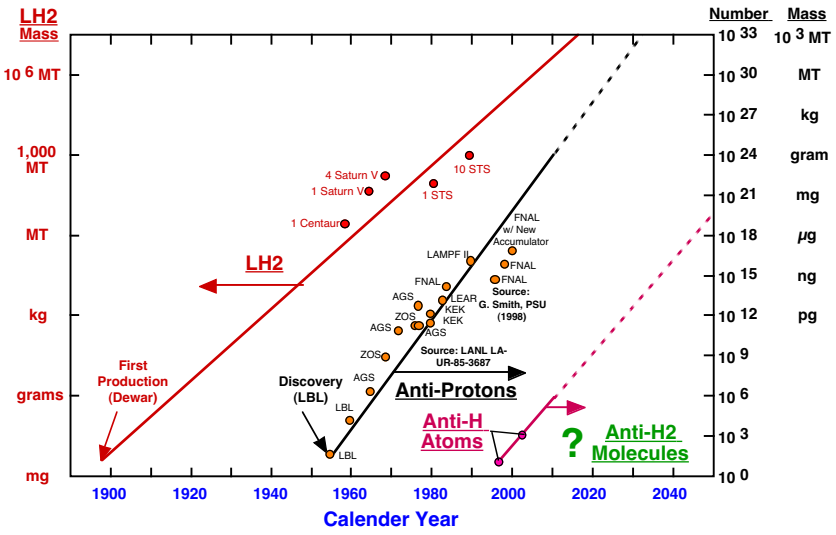

Figure 4. Comparison of Growth in Annual Production Rates of Normal-Matter LH_2 and Antimatter.

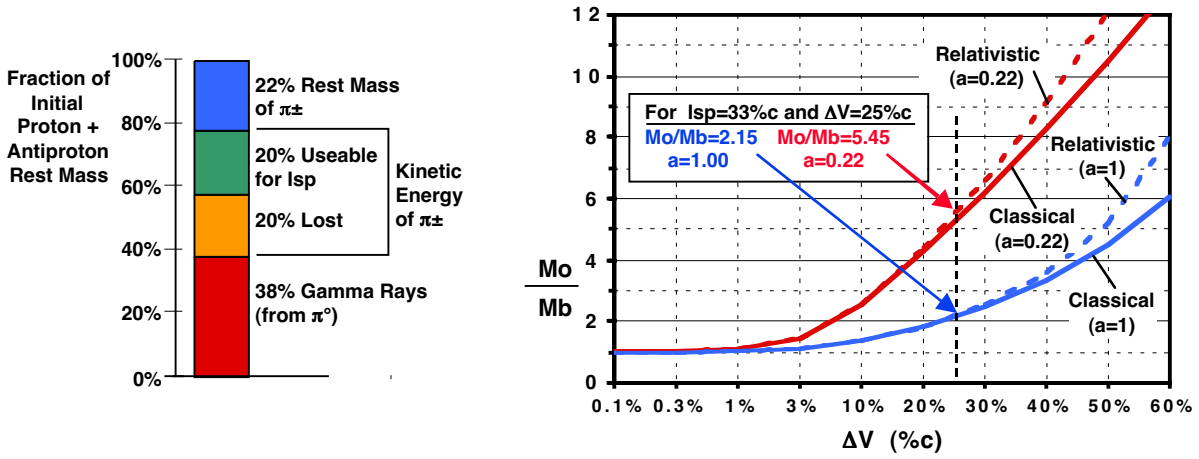

Figure 5. Comparison of Classical and Relativistic Rocket Equations with and without "Loss" of Propellant.

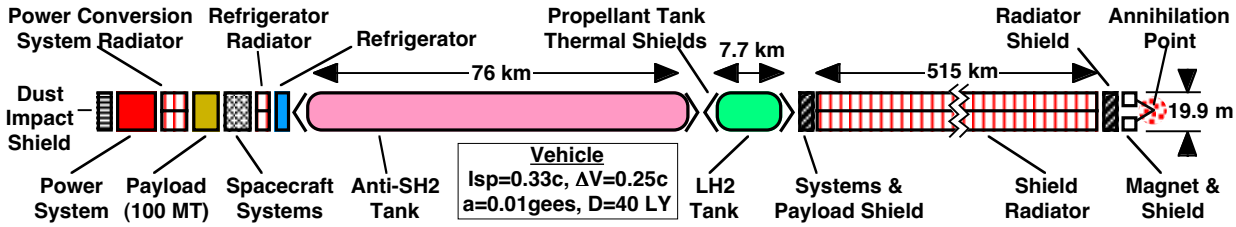

Figure 6. Conceptual Systems for an Antimatter Propulsion System.

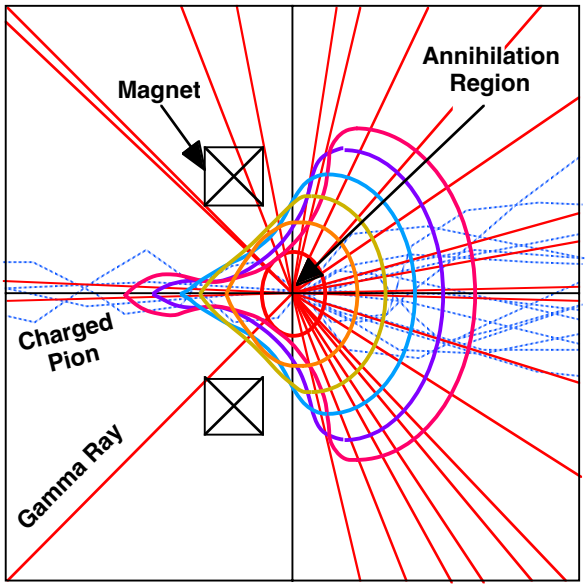

Figure 7. VISTA Magnetic Field and Monte-Carlo Simulation Results.

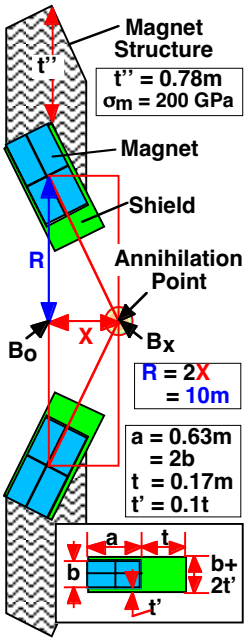

Figure 8. Magnet, Shield, and Magnet Structure Geometry.

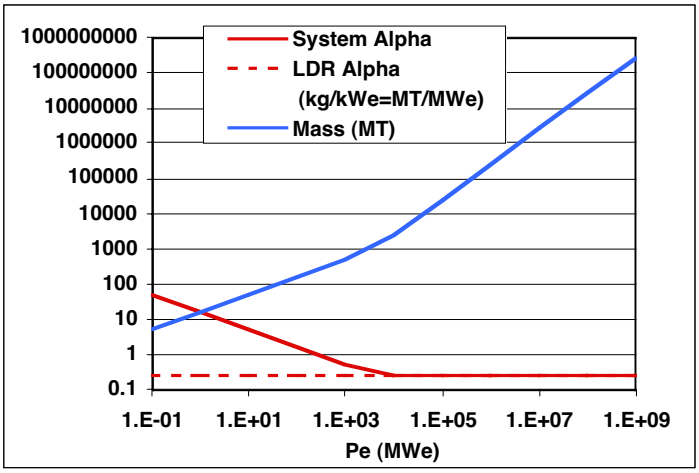

Figure 9. Variation in Electric Power System Mass and Specific Mass with Power.

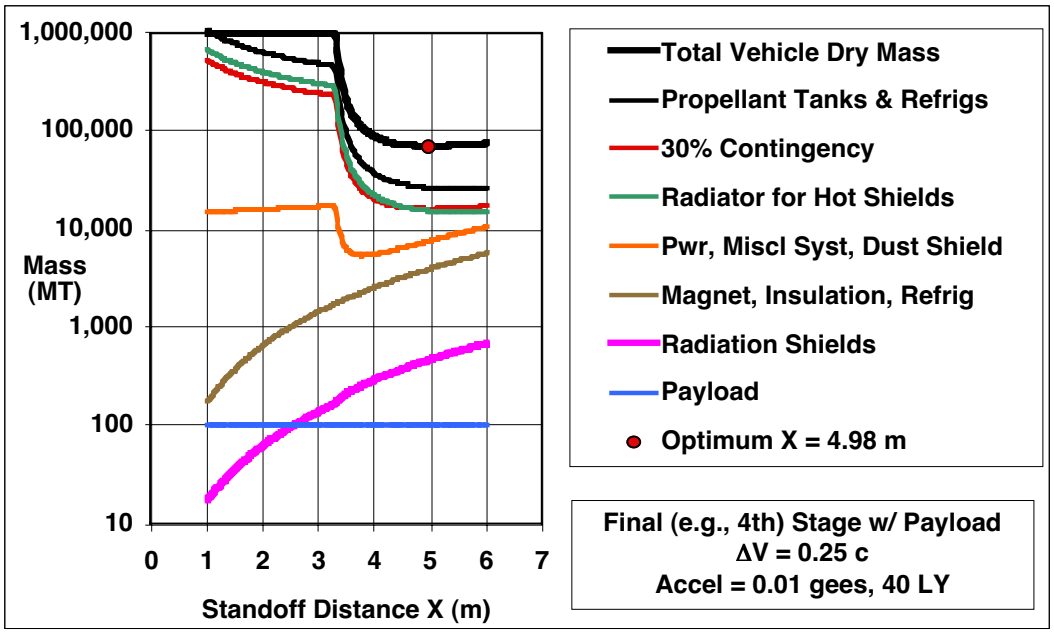

Figure 10. Variation in System Masses with Standoff Distance.

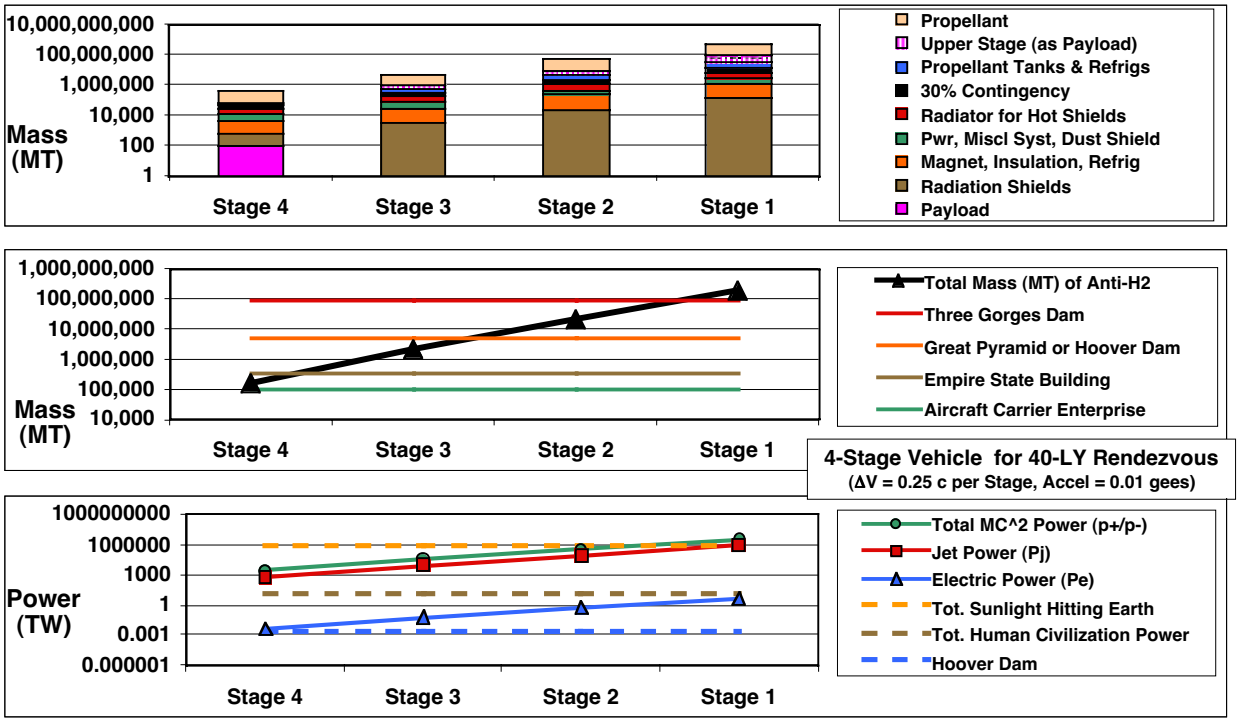

Figure 11. Four-Stage Antimatter Rocket Mass, Propellant Mass, and Power

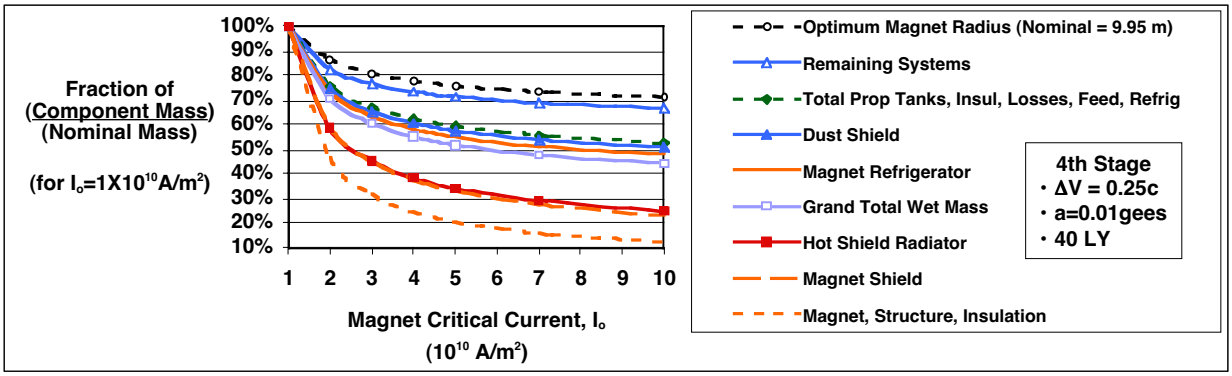

Figure 12. Reduction in Vehicle Systems with Improved Magnet Critical Current.

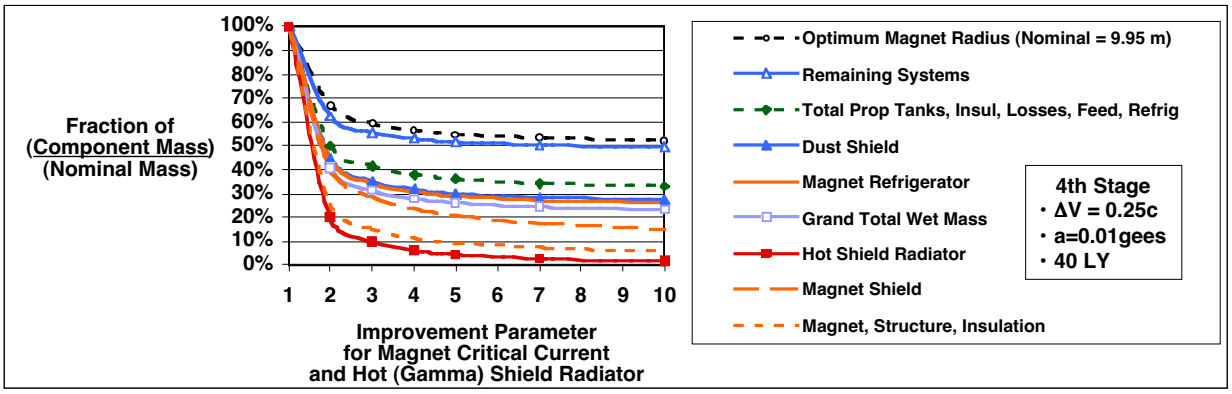

Figure 13. Reduction in Vehicle Systems with Improved Main (1500K) Radiator and Magnet Critical Current.

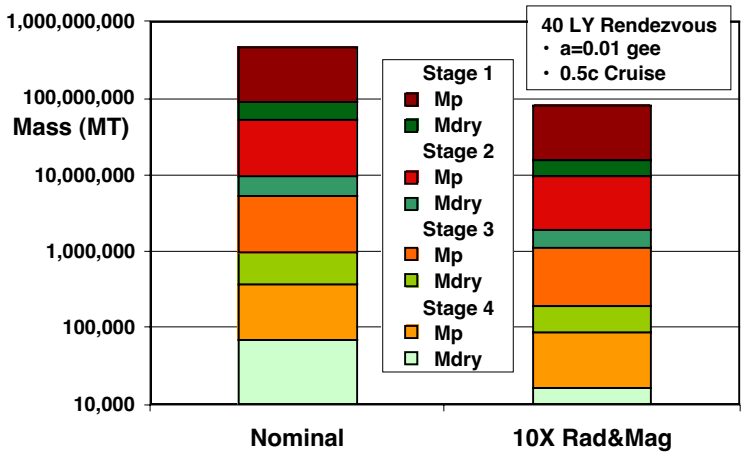

Figure 14. Reduction in Four-Stage Vehicle with Improved Main (1500K) Radiator and Magnet Critical Current.

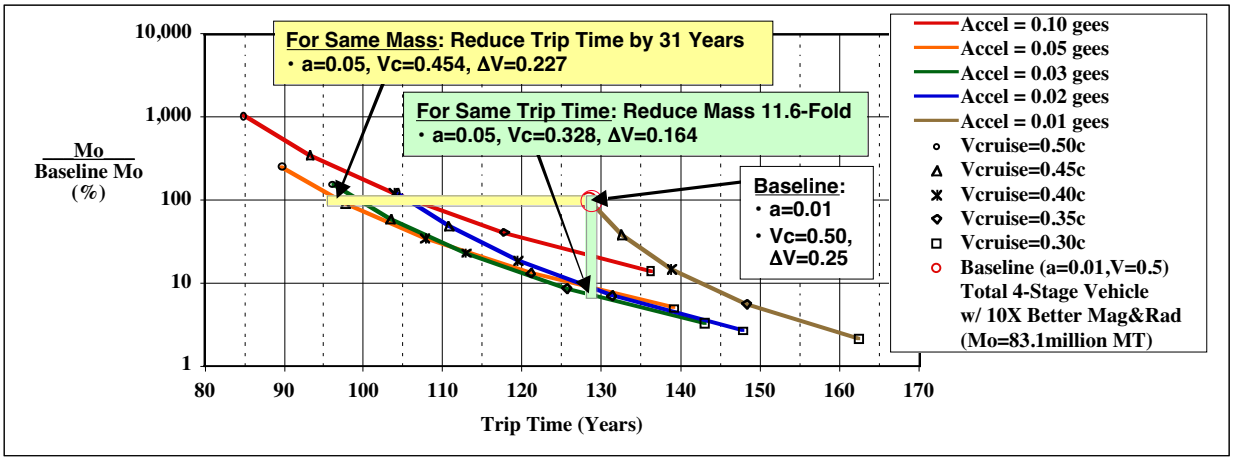

Figure 15. Tradeoffs in Acceleration, Cruise Velocity, Mass, and Trip Time.

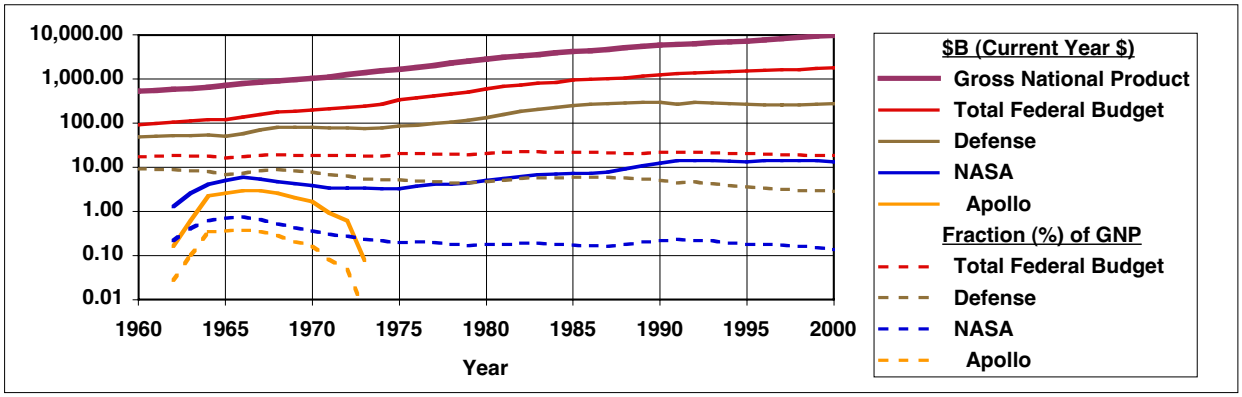

Figure 15. Comparison of NASA and Military Spending.